Titre: Title:	Study of the Hemocompatibility of Non-Woven Sub-Microfibrous Structures of Polyethylene Terephthalate (PET): Effect of Sub-Microfibres Diameter and Alignment
Auteur: Author:	Mauro Valenti
Date:	2012
Type:	Mémoire ou thèse / Dissertation or Thesis
Référence: Citation:	Valenti, M. (2012). Study of the Hemocompatibility of Non-Woven Sub-Microfibrous Structures of Polyethylene Terephthalate (PET): Effect of Sub-Microfibres Diameter and Alignment [Mémoire de maîtrise, École Polytechnique de Montréal]. PolyPublie. https://publications.polymtl.ca/1036/

UNIVERSITÉ DE MONTRÉAL

STUDY OF THE HEMOCOMPATIBILITY OF NON-WOVEN SUB-MICROFIBROUS STRUCTURES OF POLYETHYLENE TEREPHTHALATE (PET): EFFECT OF SUB-MICROFIBRES DIAMETER AND ALIGNMENT

MAURO VALENTI

DÉPARTEMENT DE GENIE CHIMIQUE

ÉCOLE POLYTECHNIQUE DE MONTRÉAL

MÉMOIRE PRÉSENTÉ EN VUE DE L'OBTENTION

DU DIPLÔME DE MAÎTRISE ÈS SCIENCES APPLIQUÉES

(GÉNIE CHIMIQUE)

DÉCEMBRE 2012

UNIVERSITÉ DE MONTRÉAL

ÉCOLE POLYTECHNIQUE DE MONTRÉAL

Ce mémoire intitulé:

STUDY OF THE HEMOCOMPATIBILITY OF NON-WOVEN SUB-MICROFIBROUS STRUCTURES OF POLYETHYLENE TEREPHTHALATE (PET): EFFECT OF SUB-MICROFIBRES DIAMETER AND ALIGNMENT

présenté par : VALENTI Mauro

en vue de l'obtention du diplôme de : Maîtrise ès sciences appliquées

a été dûment accepté par le jury d'examen constitué de :

M.TAVARES Jason-Robert, Ph.D., président

M.AJJI Abdellah, Ph.D., membre et directeur de recherche

M.JOLICOEUR Mario, Ph.D., membre et codirecteur de recherche

M.MERHI Yahye, Ph.D., membre et codirecteur de recherche

M.NAZHAT Showan, Ph.D., membre

DEDICATION

To my family

ACKNOWLEDGEMENTS

I would like to acknowledge my thesis director M. Abdellah Ajji and my co-directors M. Yahye Mehri and M. Mario Jolicoeur for their guidance and support all along the Master at Ecole Polytechnique de Montreal.

Finally, I thank all the team of doctor Merhi at Montreal Institute of Cardiology and Afra Hadjizadeh for their help and suggestions.

RÉSUMÉ

Les maladies vasculaires, particulièrement celles associées aux vaisseaux sanguins de petit diamètre, sont la première cause de décès aux États-Unis. Les coûts liés aux maladies cardio-vasculaires ont augmenté constamment avec le temps. Dans les dernières années, de nombreuses recherches en bio-ingénierie ont été réalisé afin d'obtenir une prothèse vasculaire pour les vaisseaux de petit diamètre, mais il n'y a pas encore de greffon qui a été développé et qui répond totalement aux exigences. Pour le remplacement des vaisseaux de gros diamètre, des prothèses en polyéthylène téréphtalate (PET) tissé ont été utilisées avec succès, mais elles n'ont pas pu être utilisées pour les vaisseaux de petit calibre à cause du taux d'échec élevé causé par les phénomènes thrombogéniques et l'hyperplasie myo-intimale. Les recherches effectuées précédemment ont démontré que les structures nanofibreuses en PET non-tissé produite par le procédé d'électrofilage ont des propriétés mécaniques appropriées pour leur application comme prothèse vasculaire et sont une matrice apte à la croissance des cellules endothéliales.

Dans ce mémoire, l'électrofilage sera utilisée pour la production de structures non-tissées composées de nanofibres de divers diamètres et de divers alignements. La thrombogénicité de ces structures sera testée pour sélectionner laquelle est la moins thrombogéniques pour les développements futurs.

Les structures électrofilées en PET non-tissé avec différents diamètres ont été préparées en modifiant les paramètres d'électrofilage, principalement la concentration du polymère dans la solution à électrofiler et le débit d'écoulement de la solution pendant le procédé. Le diamètre moyen des fibres augmente avec la concentration du polymère et le débit d'écoulement. Les structures sélectionnées pour les tests de thrombogénicité ont un diamètre moyen de 259 nm, 388 nm et 1148 nm.

L'orientation des nanofibres a été obtenue en changeant la vitesse de rotation du collecteur et par conséquent, la vitesse linéaire du tambour entre deux valeurs : 22,9 m/min et 114,7 m/min. L'orientation a été estimée par l'analyse visuelle des images du microscope électronique à balayage en divers endroits des structures et prises avec divers grossissements. Aucune orientation prédominante n'a été remarquée.

La thrombogénicité des structures électrofilées a été testée en analysant et mesurant l'adhésion des plaquettes humaines dans un système de perfusion qui simulait les conditions dynamiques des fluides dans les vaisseaux de petit diamètre.

L'effet de l'orientation des nanofibres sur la thrombogénicité a été évalué en analysant visuellement la forme et la distribution des plaquettes précédemment marquées en fluorescence avec un microscope confocal. Les structures avec une orientation présumée des fibres ont donné des résultats de thrombogénicité majeure par rapport aux structures sans aucune orientation de fibres. Pour cette raison, les structures électrofilées avec des fibres qu'on peut supposer orientées ont été exclues pour les tests suivants de thrombogénicité.

La thrombogénicité des structures électrofilées avec divers diamètre de fibres a été comparée en utilisant une méthode quantitative pour le calcul des plaquettes adhérées basée sur leur marquage radioactif. La relation entre le diamètre des fibres et l'adhésion plaquettaire est linéaire : la diminution du diamètre des fibres entraîne la diminution de plaquettes déposées. En outre, le dépôt des plaquettes sur la structure composée de nanofibres de diamètre moyen de 259 nm est comparable au dépôt des plaquettes sur l'endothélium intact d'une artère humaine.

ABSTRACT

The small diameter blood vessels diseases are the leading cause of death in the United States and the costs related are constantly growing. In the last years, bioengineering was applied to create a synthetic small diameter vascular graft; but a fully successful one has not been developed yet. Polyethylene terephthalate (PET) woven grafts have been used for large diameter vascular grafts, but as small calibre grafts have demonstrated low patency due to the occlusion caused by thrombogenic phenomena and myointimal hyperplasia. Previous studies report that PET nanofibrous non-woven structures have suitable mechanical properties for vascular graft application and are a suitable scaffold for endothelial cells growth.

In this dissertation, electrospinning will be used in order to produce non-woven structures composed of nanofibers with various diameters and various fibre alignments. Their thrombogenic behaviour will be tested in order to determine the best non-woven structure for future developments.

Electrospun non-woven polyethylene terephthalate structures with different fibre diameters were prepared by changing the process parameters, chiefly the polymer concentration in the electrospinning solution and the feed rate. The average fibre diameter increased increasing the polymer concentration in the solution and increasing the feed rate. The structures selected for thrombogenicity tests were composed of nanofibers with an average diameter of 259nm, 388nm and 1148nm.

The orientation of the fibres was obtained by changing the rotational collector speed and consequently the linear drum velocity between two values: 22.9 m/min and 114.7 m/min. The orientation was estimated by the visual analysis of the scanning electron microscope images taken at different magnifications and at different place of the electrospun structure. No prevalent orientation was remarked.

The thrombogenicity of the electrospun structures was tested by measuring the adhesion of human platelets in a perfusion system that simulated the small calibre fluid dynamics conditions.

The effect of the fibre orientation on the thrombogenicity was assessed visually analyzing the platelet shape and distribution after a fluorescent labelling with a confocal microscope. The

structures with supposed oriented fibres resulted in a higher thrombogenicity than the not-aligned structures. For that reason, the oriented fibre electrospun non-woven structures were excluded from following thrombogenic tests.

The thrombogenicity of the electrospun structures with different fibre diameter was compared using a quantitative method for the calculation of the adherent platelet based on their radioactive labelling. The relation between the fibre diameter and the platelet adhesion resulted linear: to a diminution of the fibre diameter corresponds a diminution of the platelet deposition. Furthermore, the platelet adhesion on the structure composed of nanofibers with an average diameter of 259 nm was comparable to the platelet deposition on the intact endothelium of a human artery.

TABLE OF CONTENTS

LIST OF TABLES

LIST OF FIGURES

LIST OF ACRONYMS AND ABREVIATIONS

ADP	Adenosine di-phosphate
CVD	Cardiovascular disease
DABCO	1,4-diazabicyclo[2.2.2]octane
DCM	Dichloromethane
EDTA	Ethylenediaminetetraacetic acid
GP	Glycoprotein
HBSS	Hank's balanced salt solution
HMWK	High molecular weight kininogen
PEG	Polyethylene glycol
PGE1	Prostaglandin E1
PET	Polyethylene terephthalate
PTFE	Polytetrafluoroethylene
PMP	Platelet microparticle
PPACK	D-phenylalanyl-L-prolyl-L-arginine chloromethyl ketone
PPP	Platelet poor plasma
PRP	Platelet rich plasma
PU	Polyurethane
SEM	Scanning electron microscope
TF	Tissue factor
TFA	Trifluoroacetic acid
TXA2	Thromboxane A2
vWF	von Willebrand factor

INTRODUCTION

Cardiovascular diseases (CVDs) are the major cause of death and disability in the world. In 2008, cardiovascular diseases caused an estimated number of 17.3 million of deaths all over the world (World Health Organisation, 2012); among them more than 800 thousands were Americans (Roger et al., 2011). The direct and indirect costs related to CVDs are constantly growing and were estimated in more than 420 billions of dollars in the only United States in 2010 (Heidenreich et al., 2011).

Among CVDs, the small diameter blood vessels diseases are the leading cause of death in United States. Blood vessels are part of the cardiovascular system and they transport the blood throughout the body. They are divided in two types: arteries, which transport the blood from the heart to the organs, and veins, which transport the blood from the organs to the heart. The Figure 1.1 shows the parts that compose both arteries and veins. The vessel wall is composed of three layers: tunica intima, tunica media and tunica adventitia. Tunica intima is divided from tunica media by the internal elastic lamina and tunica media is divided from tunica adventitia by the external elastic lamina. Tunica media is a single layer of endothelial cells, that are in contact with the blood anytime and it is the only known perfectly not thrombogenic surface. Tunica media is composed of elastic fibres and vascular smooth cells; it is the thickest layer in arteries. Tunica adventitia is made of connective tissue, rich in nerves. Even if arteries and veins wall are composed of the same components, the blood that flows in the arteries has a pressure on average 20 times higher than veins; for that reason, CVDs affect more arteries than veins. Furthermore arteries supply the heart and the brain cells, so artery diseases in some cases can lead fatal consequences.

The arteries have various diameters that become smaller from the heart to the periphery. The vessels are considered of small calibre when their inner diameter is less than 5 mm, such coronaries, cerebral and peripheral arteries. Diseases like atherosclerosis can produce the dilation, called aneurysm, or the narrowing until the occlusion, called stenosis, of small calibre arteries. The effects can be cardiac infarction in case of coronary disease, stroke if a cerebral artery is interested, and claudication if a peripheral artery is concerned.

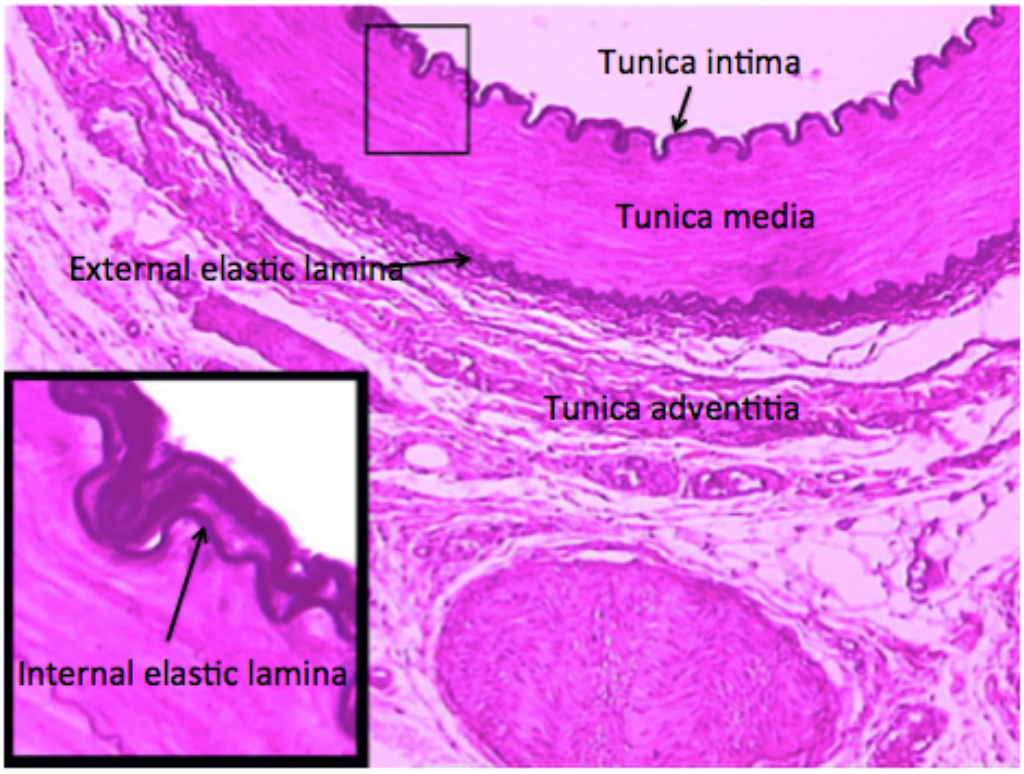

Figure 1.1 An image of the artery wall that shows tunica intima, media and adventitia and their relative thickness. Tunica are separated by an elastic lamina. Adapted from "Histology Image Bank, *The School of Medicine of the University of California, San Diego*". Reproduced with permission.

When the vascular disease is severe, the standard treatment is the bypass procedure. In 2009 were performed 416'000 bypass procedures in the United States (Roger et al., 2011). The bypass procedure consists in the creation of a blood detour that permits the supply of the tissues downstream of the vessel stenosis. Autologous vessels (above all saphenous vein and left internal mammary artery) are the gold standard for coronary and peripheral bypass procedures (Song, Feijen, Grijpma, & Poot, 2011).

Nevertheless autologous vessels are the gold standard for bypass procedures, but suitable autografts are not always available because of previous surgery or vessel damages. Moreover, mammary arteries can develop atherosclerosis plaques, and saphenous veins often develop aneurysms because of the high arterial pressure (Campbell, Efendy, & Campbell, 1999). For

these reasons, synthetic vascular prosthesis like expanded polytetrafluoroethylene (ePTFE) membranes, polyethylene terephthalate (PET) woven fibres (Dacron) and polyurethane (PU) have been investigated. Although they perform well as big and medium diameter vascular grafts, they show a lower patency than autologous grafts in small calibre vessels (Klinkert, Post, Breslau, & van Bockel, 2004). PET and ePTFE have demonstrated suitable mechanical properties for both large and small diameter vessels, but the post implantation healing responses are not physiological, producing the failure of the grafts caused by thrombosis, infection and myointimal hyperplasia. In particular, the thrombogenic phenomenon mediated by platelets causes the short-term failure of synthetic grafts, producing the occlusion of the vessel and a new surgical operation.

Various techniques have been investigated in order to improve the patency and the biocompatibility of synthetic small diameter vascular grafts; however it still doesn't exist a fully successful and anti-thrombogenic graft. In the last years nanotechnologies have opened a new window on tissue engineering techniques. Nanotechnology concerns the nanoscale manipulation, and finds lots of applications as nanofibers. The nanofiber can be defined as an elongated object with a dimension prevalent than the other two and a diameter smaller than 1000 nm. The nanofibers can reproduce the large number of nanofibrous and nanoporous biological structures that compose the human tissues; furthermore, the nanoscale functionalization of the surfaces makes possible the control of the interactions between the body and the artificial surfaces, opening new solutions for the improvement of the biocompatibility.

Many technologies have been used to obtain structures composed of nanofibers in the biomedical field: drawing (Ondarçuhu & Joachim, 1998), phase separation (Khorasani & Shorgashti, 2006), electrospinning (Agarwal, Wendorff, & Greiner, 2008; Xie, Li, & Xia, 2008). However the electrospinning have demonstrated to be more suitable; as a matter of fact, the electrospinning technique is simpler, more versatile and cheaper.

Electrospun non-woven nanofibrous structures have demonstrated to have mechanical attributes suitable for small diameter vascular replacement (Hadjizadeh, Ajji, & Bureau, 2011). In addition, the electrospun structures are characterized by a large surface area, high porosity and interconnected pores, that enhance the endothelial cells proliferation and viability (Ma, Kotaki, Yong, He, & Ramakrishna, 2005).

In order to produce nanofibrous structures, the electrospinning technique, the applications of polyethylene terephthalate in the biomedical field, the reactions of the blood when it gets in contact with a foreign object, and the mechanism that lead to the formation of a thrombus will be deepened.

CHAPTER 1 LITERATURE REVUE

In this chapter, the electrospinning technique, the applications of polyethylene terephthalate in bioengineering and the blood reactions that lead to the thrombogenic phenomena will be investigated. Beside the description of the electrospinning technique, a literature review of the effect reported by other researchers of the electrospinning parameters on the fibres that compose the non-woven structures will be presented. Afterwards, the PET features and the actual applications of PET as biomedical material will be presented. Finally, the mechanisms that lead to the thrombogenic phenomenon will be deepened: coagulation, complement, platelet and leukocyte activation.

1.1 Electrospinning

We can define the electrospinning as the process that creates fibres through an electrically charged jet of polymer solution. The first patent relating to the electrospinning was registered and copyrighted by Anton Formhals in 1934 (Formhals, 1934). In Figure 1.1 we can appreciate the simplest electrospinning setup: a pipette full of polymer solution, DC voltage supply with two electrodes, and a collector. One of the electrodes is inserted in the pipette and it's charged at a high voltage in order to charge the solution. The repulsion of the charges at the surface works against the surface tension and deforms the droplet exiting the needle tip into a conical shape, called Taylor Cone. When the charge density is high enough the cone becomes unstable and a jet of charged solution is emitted from the needle to the grounded collector. During the path between the needle and the collector the jet is accelerated, stretched and dried, resulting in nanofibers when it reaches the collector.

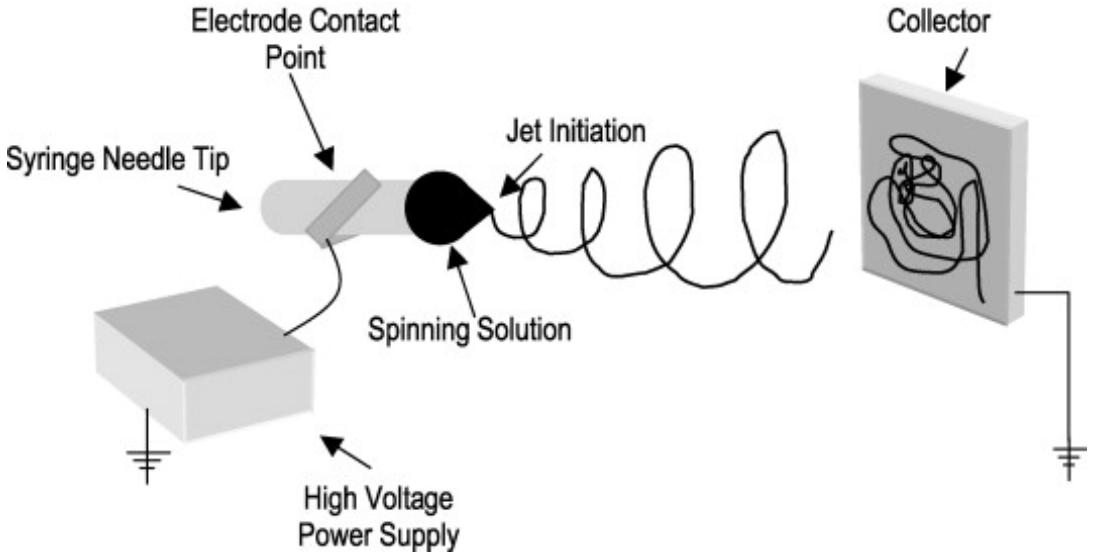

Figure 1.1 The basic electrospinning setup, composed of a syringe full of the electrospinning solution, a high voltage supply with two electrodes, and a collector. Boland, E. D., Matthews, J. A., Pawlowski, K. J., Simpson, D. G., Wnek, G. E., & Bowlin, G. L. (2004). Electrospinning collagen and elastin: Preliminary vascular tissue engineering. *Frontiers in Bioscience, 9(2),* 1422-1432. Reproduced with permission.

Despite the simplicity of the setup, a lot of controllable parameters affect the process, making the electrospinning a useful technology to obtain a lot of structures with different morphologies and properties. In particular, the parameters affect the resulting structures in two ways: they affect the type and the diameter of the electrospun fibres and the patterning of the non-woven structure obtained. About the fibre properties, the main parameters that affect the process are:

- polymer solution properties;
- processing conditions;
- ambient parameters.

On the other hand, the most important parameter that influences the patterning of the non-woven electrospun structures is the type of collector.

1.1.1 Polymer solution properties

The properties of the polymer solution have the most important effect on the electrospinning process and fibre shape and dimensions. For that reason, when we chose the polymer and the solvents for the electrospinning, their properties have been studied in order to obtain the most suitable non-woven structure for our application. The most important properties of the polymer solution are:

- polymer molecular weight;
- solution viscosity;
- surface tension;
- solution conductivity.

1.1.1.1 Molecular weight

The most important feature of the polymer is the molecular weight. It represents the length of the polymer chain that influences the viscosity of the solution. This is the first parameter to be taken into account for the effect on the solution viscosity, so on the electrospun fibres.

1.1.1.2 Solution viscosity

The viscosity of the solution is another important parameter that affects the dimension of the electrospun fibres. It depends on the number of entanglements between the polymer chains in the solution. The viscosity of the solution affects the diameter dimension of the fibres in the following manner: to a higher viscosity corresponds a larger fibre diameter (Baumgarten, 1971) (Deitzel, Kleinmeyer, Harris, & Beck Tan, 2001).

The two parameters that influence the viscosity are: the molecular weight of the polymer and the concentration of the polymer in the solution. There is a lower and a upper limit in the number of entanglements, i.e. in the viscosity of the solution, that permits the continuity of the jet during the electrospinning; as a matter of fact a low viscosity can bring the jet to break into droplets or can result in beaded fibres after the deposition on the collector because in this case the dominant

influence on the electrospinning jet is the surface tension (Shenoy, Bates, Frisch, & Wnek, 2005). On the other hand, if the concentration of the polymer is too high it is difficult to pump the solution through the needle and the fast evaporation of the solvent can plug the needle tip (Zong et al., 2002). Furthermore, the diameter of the fibres depends on the interaction between the solution and the charges, so when viscosity is low the charges are able to fully stretch the solution jet and often there is the formation of secondary jets that are stable enough to deposit on the collector fibres with smaller diameter (Eda, Liu, & Shivkumar, 2007) (Reneker, Yarin, Fong, & Koombhongse, 2000). Finally, the concentration of the polymer in the solution yields to different deposition areas, in fact to a higher viscosity corresponds a smaller deposition area.

1.1.1.3 Surface tension

In order to start the electrospinning of the solution, it is necessary that the electrical force that stretches the charged solution overcomes the surface tension. For that reason, it's an important parameter that affects the stability of the process and the shape of the fibres.

The surface tension is the tendency of a liquid to decrease the surface area per unit mass. In order to avoid the formation of beads in the fibres it is necessary that the charges stretch the jet overcoming the surface tension, so that the solvent molecules don't aggregate adopting a spherical shape (Fong, Chun, & Reneker, 1999). This behaviour depends on the number of entanglements between the polymer chains and the solvent molecules, so when the viscosity of the solution is high, the solvent molecules tend to spread over the polymer molecules preventing their aggregation. Often, it's needed to reduce the surface tension to start electrospinning so a solvent such as ethanol or a surfactant can be added to the solution.

1.1.1.4 Solution conductivity

The electrospinning process needs the stretching of the solution caused by the repulsion of the charges at its surface. The conductivity is the ability of the solution to conduct electricity, so it depends on the number of free ions in the solution.

The number of charges carried by the electrospinning jet influences the stretching of the jet,

modifying the diameter and the shape of the fibres. When the solution conductivity augments, the diameter of the fibres decreases (Son, Youk, Lee, & Park, 2004), the critical voltage for electrospinning diminishes and the deposition area increases. In order to increase the solution conductivity a salt or an ionic surfactant can be added, as the last one reduce also the surface tension.

1.1.2 Processing conditions

After choosing the polymer and the solvents as the most worth fit for our application, various process conditions affect the electrospinning process. Some of them are simply manageable and have a big effect on the resulting electrospun structures:

- voltage;
- feed rate;
- needle diameter;
- distance between tip and collector.

1.1.2.1 Voltage

As mentioned before, the crucial element in electrospinning is the induction of the charges in the solution produced by the voltage supply and the formation of an electric field between the syringe and the collector. Under these two effects, the electrospinning process starts when the electrostatic force in the solution overcomes the surface tension of the solution.

Both a negative or a positive voltage can be applied and starting from 6 kilovolts the voltage is strong enough to cause the distortion of the solution drop at the tip of the needle into the shape of a Taylor Cone (Taylor, 1969). The stability of the Taylor Cone and consequently the continuity of the electrospinning process depend on the good balance between feedrate of the solution and voltage, that can reach tens of kilovolts. At higher voltage the jet is accelerated by the great amount of charges so that more volume of solution is drawn from the needle, resulting in a smaller and less stable Taylor Cone; sometimes it withdraws into the needle (Deitzel et al., 2001)

As the voltage supply has the role of stretching the jet, it has a big influence on the morphology of the fibres. When a high voltage is applied the resulting greater stretching of the fibres produces the reduction of the fibres diameter and a faster solvent evaporation (Megelski, Stephens, Chase, & Rabolt, 2002). Furthermore, a higher voltage coupled with a solution with a low viscosity produces secondary jet with the consequence of reducing the fibre diameter (Demir, Yilgor, Yilgor, & Erman, 2002). At the same time, some authors have reported the formation of beads and their increased density at a higher voltage, probably due to an increased instability of the Taylor Cone (Deitzel et al., 2001) (Zong et al., 2002).

1.1.2.2 Feedrate

The feedrate determines the amount of solution exiting the needle, that must be the same amount of solution that have to be deposited on the collector in order to obtain a stable Taylor Cone. In Figure 1.2 we can appreciate the different Taylor cone shapes and the resulting different diameter electrospun fibres by changing feedrate and voltage parameters. When feedrate is increased the fibre diameter increases, because a greater amount of solution is drawn away from the needle tip (Hadjizadeh et al., 2011). However, when the feedrate increases, the jet takes more time to dry and the fibres deposited may have a residual solvent that can bring the fibres to fuse together or to form beads (Yuan, Zhang, Dong, & Sheng, 2004).

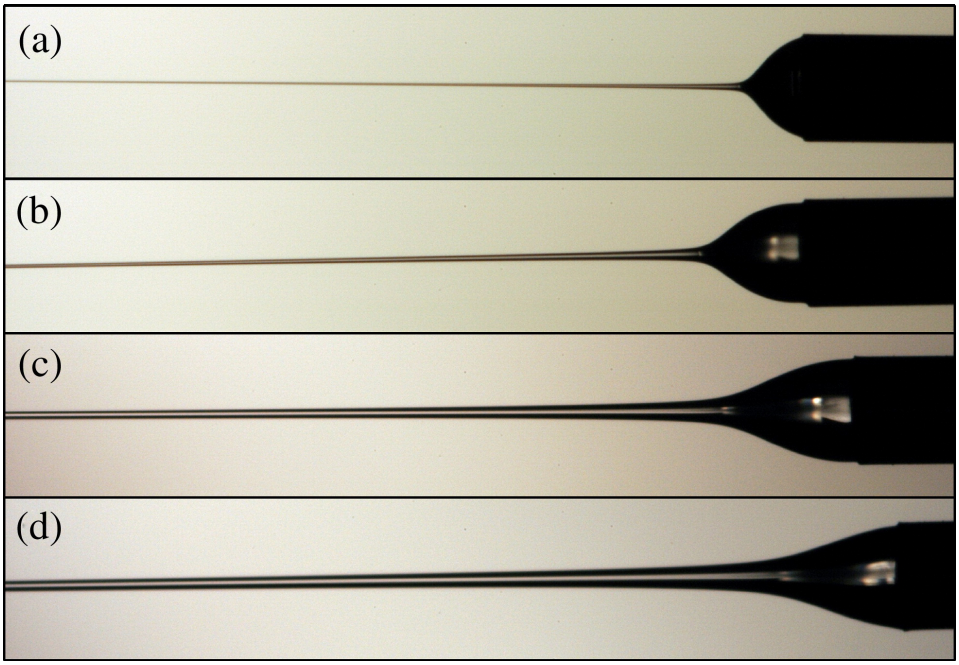

Figure 1.2 Four different Taylor Cone and the resulting fibres shape. The feedrate has been increased from (a) to (d) adjusting the voltage only for stabilize the jet and leaving the other conditions the same. Rutledge, G. C., & Fridrikh, S. V. (2007). Formation of fibers by electrospinning. *Advanced Drug Delivery Reviews, 59*(14), 1384-1391. Reproduced with permission.

1.1.2.3 Needle diameter

The needle diameter has a certain effect on the electrospinning process and particularly on the fibre diameter of the non-woven structure. The needle diameter, in fact, influences the size of the droplet at the tip of the needle. If the needle is too big or too small electrospinning process is not possible, because in the first case more solution is exposed to the air before electrospinning process stabilizes resulting in the plugging of the needle, while in the second case the extrusion of the solution is too difficult (Mo, Xu, Kotaki, & Ramakrishna, 2004). Furthermore, the dimension of the droplet influences its surface tension, so when the droplet is smaller it is needed a greater electrostatic force in order to start the jet; the effect is that the solution is stretched for a longer time, resulting in smaller diameter fibres.

1.1.2.4 Distance between tip and collector

The distance between tip and collector has an effect on the electrospun fibres morphology because it affects the flight time of the solution and the electric field strength. If the distance is low, the electric field is stronger and the flight space is shorter, so that the jet is accelerated and the solvent doesn't have the time to evaporate; this phenomenon produces the merging of the fibres and a network structure or the formation of beads because the electric field is too strong (Deitzel et al., 2001).

Changing the distance between tip and collector has also an effect on the fibre diameter, but two contrasting behaviours have been reported. Increasing the distance results in a diminution of the fibre diameter when the flight time of the jet is increased, letting the solution to be more stretched by the electrostatic field (Zhao, Wu, Wang, & Huang, 2004); in other cases the fibre diameter augmented because the electric field strength decreases resulting in a less stretching of the jet (Lee et al., 2004).

1.1.3 Ambient parameters

The electrospinning process is influenced by a lot of parameters, as it has been shown before. Some parameters are directly linked to the solution and the electrospun setup, and the features of the surrounding environment are other parameters.

Two ambient parameters have the most important effect on the morphology of the fibres:

- temperature;
- humidity.

1.1.3.1 Temperature

The temperature has an important effect on solvent evaporation, viscosity and solubility of the polymer in the solvent. If the temperature increases the solubility of the polymer in the solvent increases, the same for the viscosity of the solution and the evaporation rate of the solvents (De Vrieze et al., 2009); for that reason, the temperature is an important parameter in the

electrospinning process and influences significantly the fibre morphology.

1.1.3.2 Humidity

The humidity of the electrospinning environment influences the electrospinning process in two ways: the water condensation around the fibres and the rate of evaporation of the solvent. Water condensation can produce pores on the fibre surface (Casper, Stephens, Tassi, Chase, & Rabolt, 2003). On the other hand, the evaporation rate depends on the humidity. At a low humidity, the evaporation of the solvents is very fast, and at the limit, risks to plug the needle tip in the first steps of electrospinning; while at a high humidity the evaporation is insufficient and the electrospinning jet is not dry when it reaches the collector, making the fibres to fuse together. In a certain range, increasing humidity decreases the fibre diameter because the evaporation rate decreases enough to elongate the jet for a longer time, without producing the fibre fusion on the collector (De Vrieze et al., 2009; Tripatanasuwan, Zhong, & Reneker, 2007).

1.1.4 Patterning

In the previous sections, the effect of the parameters on the electrospun fibres has been discussed, but it is important to discuss also the surface features of the structure, such as patterning of the non-woven structures.

In order to increase the application fields of the electrospinning process it is important to control the fibre deposition, because the interaction between the electrospun structures and the human body depends on the patterning of the fibres. A lot of studies have been carried out in order to investigate the effect of different collectors on the patterning of the fibres. The collector that we used in this research was a smooth cylindrical collector.

A cylindrical collector has two advantages compared to plate collectors: first of all, it permits to obtain aligned fibres when it turns at high speed and, on the second hand, permits to obtain non-woven structures with uniform thickness along one direction. The alignment of the fibres is possible when the rotating speed of the collector is high enough to take up the electrospun fibres on the surface of the collector and wound around it. In Figure 1.3 different alignment degree for

polyethylene terephthalate electrospun fibres were obtained as shown by changing the rotating and the translating speeds of the collector (Hadjizadeh et al., 2011).

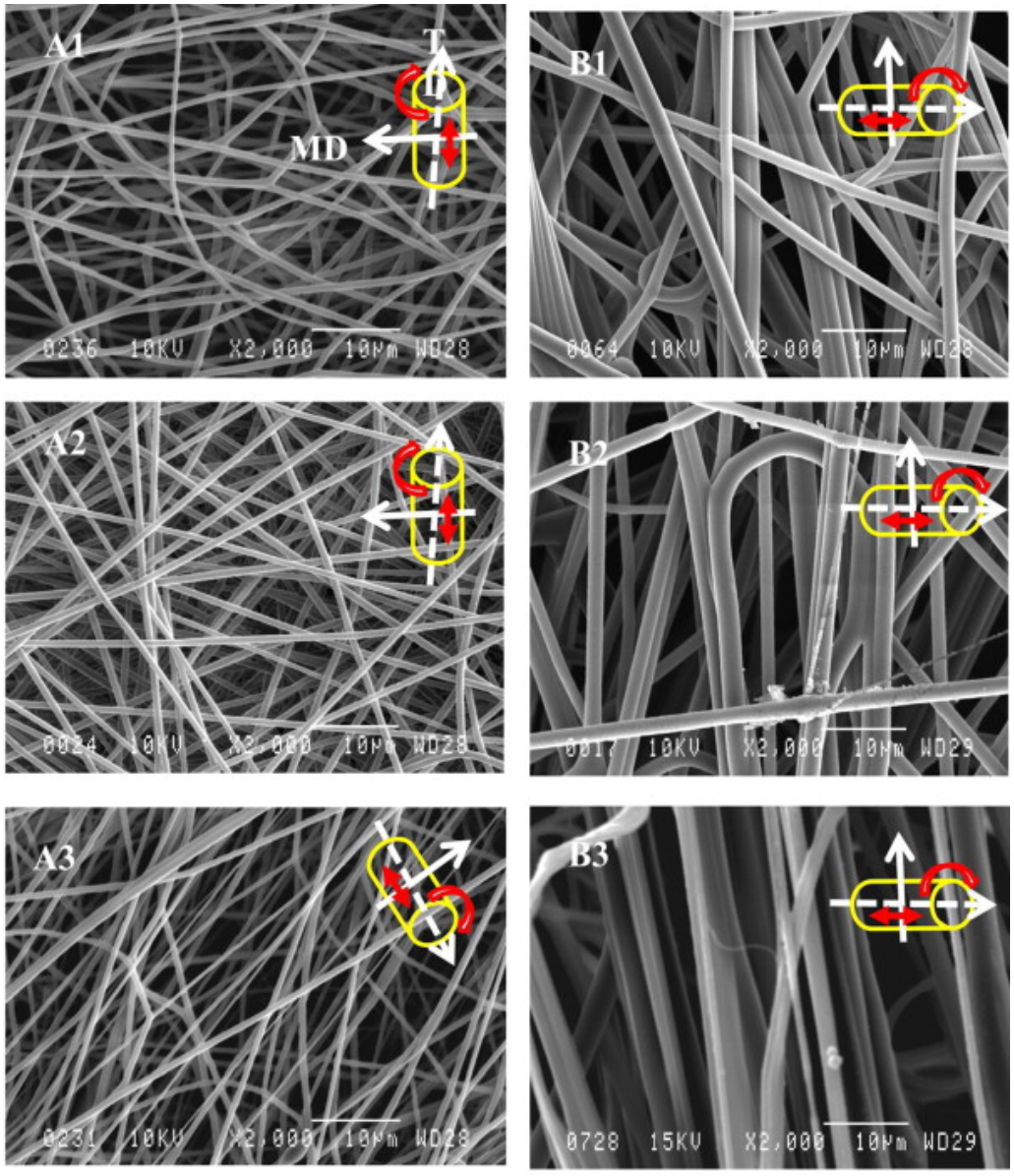

Figure 1.3 Images taken with scanning electron microscopy (SEM) showing the alignment degree of two different diameter polyethylene terephthalate electrospun fibres (A1 to A3: Diameter=0.7 μm Feedrate=0.5mL/h and B1 to B3: Diameter=1.2 μm Feedrate=10mL/h) changing the drum linear velocity and the translating velocity of the collector. A1&B1 Drum linear velocity (MD) = 22.5 m/min Translating velocity (TD) = 0.3 m/min; A2&B2 MD = 36

m/min TD = 1 m/min; A3&B3 MD = 36 m/min TD = 0.3 m/min. Hadjizadeh, A., Ajji, A., & Bureau, M. N. (2011). Nano/micro electro-spun polyethylene terephthalate fibrous mat preparation and characterization. *Journal of the Mechanical Behavior of Biomedical Materials, 4*(3), 340-351. Reproduced with permission.

1.2 Application of electrospinning and PET in bioengineering

As explained in sub-section 1.1 the electrospinning is a versatile technique, it permits in fact to obtain a wide range of non-woven structures made of nanofibers with a relatively simple set up and in a large scale production. The nanofibers obtained with the electrospinning technique have demonstrated to adapt in lots of applications as filters (Qin & Wang, 2006), as reinforcing component in composite materials (Zucchelli, Focarete, Gualandi, & Ramakrishna, 2011), as textile materials(Kang, Park, Kim, & Kang, 2007), as plant protectors in the agronomic field (Bansal, Bubel, Agarwal, & Greiner, 2012) and many others. However, the most important application field of electrospinning technique is nanobioengineering.

Nanobioengineering is a branch of bioengineering wherein nanofibers are used in order to reproduce the large number of nanofibrous and nanoporous biological structures that compose the human tissues.

In the biomedical field, the non-woven nanofiber structures have been used for many applications that can be summarized in three main utilization fields:

- wound dressing;
- drug delivery;
- tissue engineering.

In this dissertation, the application of tissue engineering of vascular grafts will be deepened. As a matter of fact, electrospinning have demonstrated to be a simple technique, versatile, cheap and reproducible.

Nowadays many technological solutions have been found for the artificial substitution of large diameter vessels, based on the utilization of woven structures in polyethylene terephthalate (PET)

and polytetrafluoroethylene (PTFE); but for small diameter vessels no valid solutions have been found.

As mentioned before, the PET has already been used as vascular graft for large diameter vessels. The PET features that make it suitable for vascular graft applications are:

- biostability;
- possibility of surface modification;
- mechanical properties;
- cost-effectiveness.

1.2.1 Biostability

Vascular prosthesis in PET have demonstrated to have a good long-term patency, because of PET biostability. In particular, PET is not subjected to significant chemical degradation in the biological environment and the long-term mechanical failure that have been counted for Dacron® large diameter prosthesis are only due to fabrics imperfections and design errors (Dieval et al., 2012).

1.2.2 Surface modification of PET

A lot of researches have been carried out about the surface modification of PET. Electrospun PET nanofibers can be functionalized in many ways in order to improve the biocompatibility of the material (Ma et al., 2005). Among the others, the improvement of the hemocompatibility of PET is possible with three strategies of coating: with drugs, natural proteins or artificial polymers. Among drug delivery systems, there are active agents attachment, such as anticoagulant, antithrombotic, antibiotic drugs, that can be attached to PET by various techniques (heparin binding, silver ions binding, plasma polymerization, etc.) (Blanchemain et al., 2005).

On the other hand, natural proteins and artificial polymers such collagen coating (Ma, Mao, & Gao, 2007) and gelatine coating (Liang, Hsiao, & Chu, 2007), or polyethylene glycol (PEG) coating (Dimitrievska et al., 2011) and others, can be used in order to functionalize the PET surface.

1.2.3 Mechanical properties

The mechanical properties of electrospun PET structures have been investigated by Hadjizadeh et al., and it has been demonstrated that electrospun PET nanofiber structures are mechanically suitable for small diameter vascular prosthesis (Hadjizadeh et al., 2011).

As explained before, nowadays doesn't exist a suitable small diameter vascular graft, but as PET is a suitable material for vascular prosthesis and electrospinning is a technology used in bioengineering, we will try to electrospin PET to solve the thrombogenic problems of the actual grafts. For that reason, a better understanding of the failure causes and the blood mechanisms occurring is necessary in order to design a better graft.

1.3 Hemocompatibility

Hemocompatibility is defined as "the ability of a biomaterial in contact with circulating blood to perform with an appropriate response related to its specific application" (Translation Bureau. Government of Canada, 2012a). The definition is very generic, so it must be specified for every application. In our study, the biomedical devices of interest are synthetic small diameter vascular prosthesis. Accordingly, we must define the "appropriate response" to these specific biomaterials. Although fundamental patterns of blood activation have been uncovered and various promising passivation schemes for blood contacting materials have been suggested, a complete picture of the involved activation mechanisms and perfectly hemocompatible engineered surfaces are still to be achieved.

Despite many studies made on the materials of vascular grafts, nowadays, the failure of small diameter artificial vascular grafts is still frequent and there is no material that is optimal and suitable for this application. The major reason that leads to the failure of small diameter polyethylene terephthalate (Dacron) and polytetrafluoroethylene (Teflon) vascular grafts is the occlusion (Bergan et al., 1982) (Pevec, Darling, L'Italien, & Abbott, 1992), which is related to two main reasons:

- poor hemodynamics;
- thrombogenicity.

1.3.1 Hemodynamics

The hemodynamic parameters have an effect on the occlusion phenomena that occurs in small diameter vascular grafts. Indeed, large diameter vascular grafts have a different behaviour than small diameter ones. Nowadays, a big challenge in our attempt to reduce the failure of vascular grafts is to reduce the radial compliance mismatch between the graft and the native vessel at anastomoses. The mismatch, as a matter of fact, causes intimal hyperplasia and as consequence the occlusion of the graft (Crapo & Wang, 2010). In addition, differences in shear stresses between large and small diameter vessels are very different and influence the interactions of blood cells and proteins with the surfaces. Shear stress increases with reduced diameter and increased blood flow and has an important impact on the coagulation cascade (Basmadjian, Sefton, & Baldwin, 1997), platelet aggregation (O'Brien, 1990) and leukocyte activation.

1.3.2 Thrombogenicity

In this dissertation, we will present the behaviour of the blood when it comes in contact with an artificial material, such as a vascular graft. The reactions involve blood proteins and cells, and could lead to the formation of thrombi, which depends on the thrombogenicity of the surfaces.

Thrombogenicity is defined as the property of a substance to cause the formation or the development of a blood clot or thrombus within the vascular system (Translation Bureau. Government of Canada, 2012b). When a foreign surface is exposed to blood, complex series of events occur, which include:

- water adsorption;
- protein adsorption;
- platelet activation and adhesion;
- leukocyte activation and adhesion;

- activation of complement;
- coagulation.

In Figure 1.4 the components that participate in the thrombogenic phenomenon are summarized. Leukocyte and complement activation are normally referred as the inflammation reaction to a foreign surface, but they also have a role in the formation of thrombi (Gorbet & Sefton, 2004).

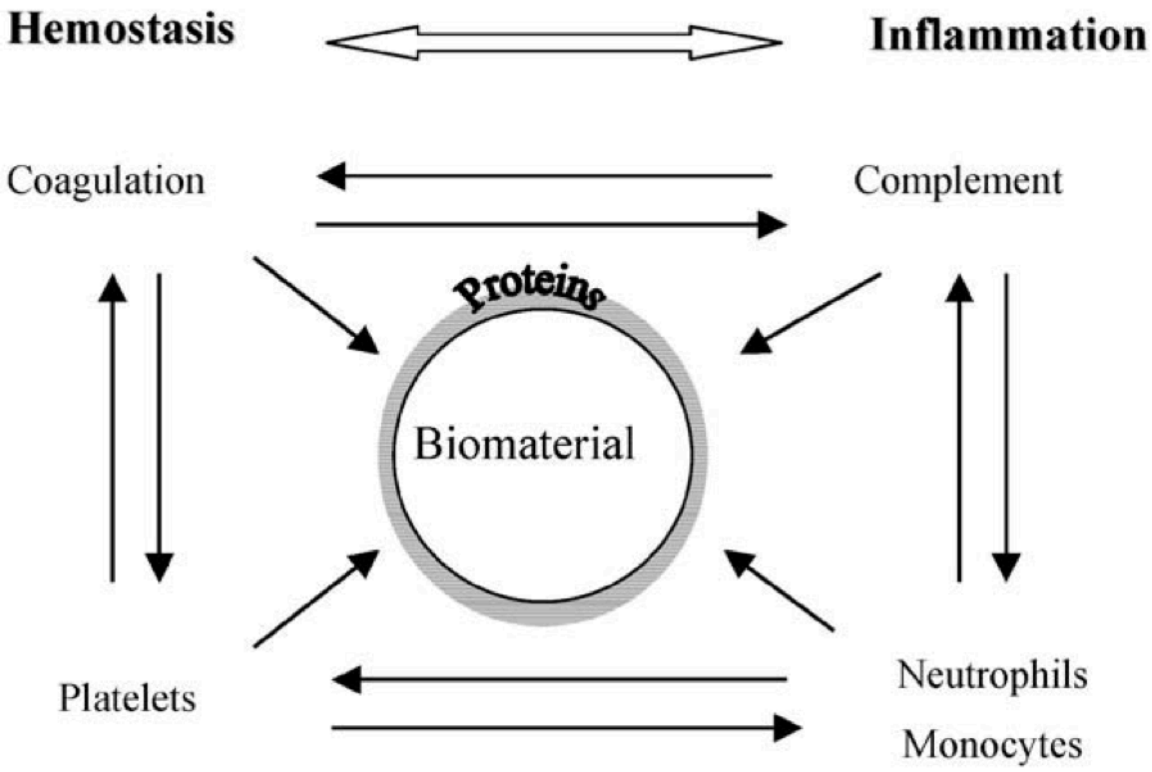

Figure 1.4 The components relevant to thrombosis. Gorbet, M. B., & Sefton, M. V. (2004). Biomaterial-associated thrombosis: roles of coagulation factors, complement, platelets and leukocytes. *Biomaterials, 25*(26), 5681-5703. Reproduced with permission.

1.3.2.1 Water adsorption

The first event that occurs on the biomaterial after implantation in the vascular system is the

adsorption of water molecules and inorganic ions found in the plasma. Different interactions of water molecules happen on hydrophilic and hydrophobic surfaces (Vogler, 1998), but in both cases the interaction is immediate and has a role in the following adsorption of proteins interfering with their functional groups.

1.3.2.2 Protein adsorption

As mentioned before, the reaction that immediately follows the water adsorption on the biomaterial is the selective and competitive adsorption of plasma proteins (Horbett, 1993). Plasma proteins are transported at the surface of the biomaterial, they react with the surface and finally they are subjected to a conformational change. The reaction between the protein and the surface is dependent on the type of surface; there are three main types of bonds: electrostatic bonds when the surface has charged sites, hydrogen bonds with polar surfaces and hydrophobic interactions with non-polar or low polar materials (Zhang, 2004). Every protein has an affinity with the blood cells and with the activation of the coagulation or the complement systems, so they influence the thrombogenicity of the artificial surfaces. In general, albumin, which is the most abundant plasma protein, is considered as a thrombo-resistant protein; whereas fibrinogen is a thrombogenic protein because it is involved in platelet adhesion and aggregation, and is the precursor of fibrin in the coagulation cascade.

1.3.2.3 Platelets

Platelets are small, anuclear cells with a diamter of 2-3 μm derived from the fragmentation of megakaryocytes. The physiological role of platelets, in primary hemostasis, is to preserve the integrity and continuity of the vascular wall, forming platelet clots if the vessel is damaged. Beyond their role in hemostasis, platelets have emerged as active players in inflammation as well as modulators of the immunological system.

Platelets become activated after their contact with any thrombogenic surface, such as collagen and von Willebrand factor (vWF) of the sub-endothelial surfaces, as well as the structures of artificial surfaces. The activation of the platelets is mediated by the binding of a ligand to its receptors on the platelet membrane. A lot of agents present in the blood and on the vascular wall

surface are potent platelet agonists, which include thrombin, collagen, vWF and others (Blockmans, Deckmyn, & Vermylen, 1995). Thrombin activates platelets via its binding to the protease activator receptors on the platelet surfaces. Collagen contributes to platelet adhesion and activation via its binding to a glycoprotein, named GPIa/IIa, whereas vWF mediates its action on platelet via its binding to GPIb.

Platelets activation induces a series of signalling reactions that lead to subsequent physiopathological reactions. First of all, platelet activation is followed by the release and secretion of their dense and alpha granules. Among the substances released by activated platelets, adenosine di-phosphate (ADP) is a platelet agonist that contributes to enhance platelet activation and aggregation at the site of vascular injury. In addition, the glycoprotein P-selectin, that is expressed on the platelet membrane following platelet activation, is considered as a thrombo-inflammatory molecule because it mediates the interaction of platelets with leucocytes (Rinder, Bonan, Rinder, Ault, & Smith, 1991). The activation of platelets initiates also the production of thromboxane A2 (TXA2), which is involved in the activation and recruitment of other platelets (FitzGerald, 1991). Platelet activation and release reactions are followed by changes in platelet shape forming filopodia and lamellipodia, and start to aggregate at the injured or thrombogenic vascular surfaces, forming the so-called white thrombus, a platelet plug with fibrin clot, as schematized in Figure 1.5.

Finally, activated platelets loose small fragments of their membranes in the blood, called platelet microparticles (PMP), that adhere to fibrinogen and fibrin and have an important pre-coagulant activity (Italiano, Mairuhu, & Flaumenhaft, 2010).

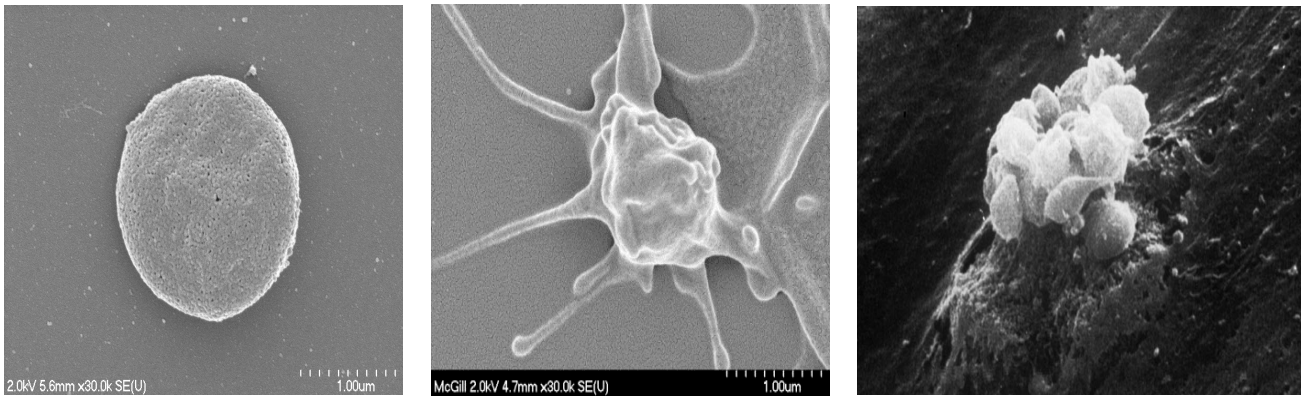

Figure 1.5 Scanning electron microscopy images of platelet shape change and aggregation. Left: Resting platelet. Middle: Activated platelet. Right: Aggregated platelets. Images are courtesy of Dr. Merhi. Reproduced with permission.

1.3.2.4 Coagulation

The coagulation of blood is a complex phenomenon that involves many enzymes and proteins. There are two pathways, intrinsic and extrinsic, that bring both to the formation of a fibrin clot. The common final stage is the formation of the clot made of fibrin that originates from the cleavage of fibrinogen made by thrombin. After this stage, the activation of Factor XIII stabilizes the fibrin clot and transforms it in a thrombus with aggregated platelets. Figure 1.6 illustrates the coagulation cascade with the intrinsic and extrinsic pathways and the enzymes involved in the process.

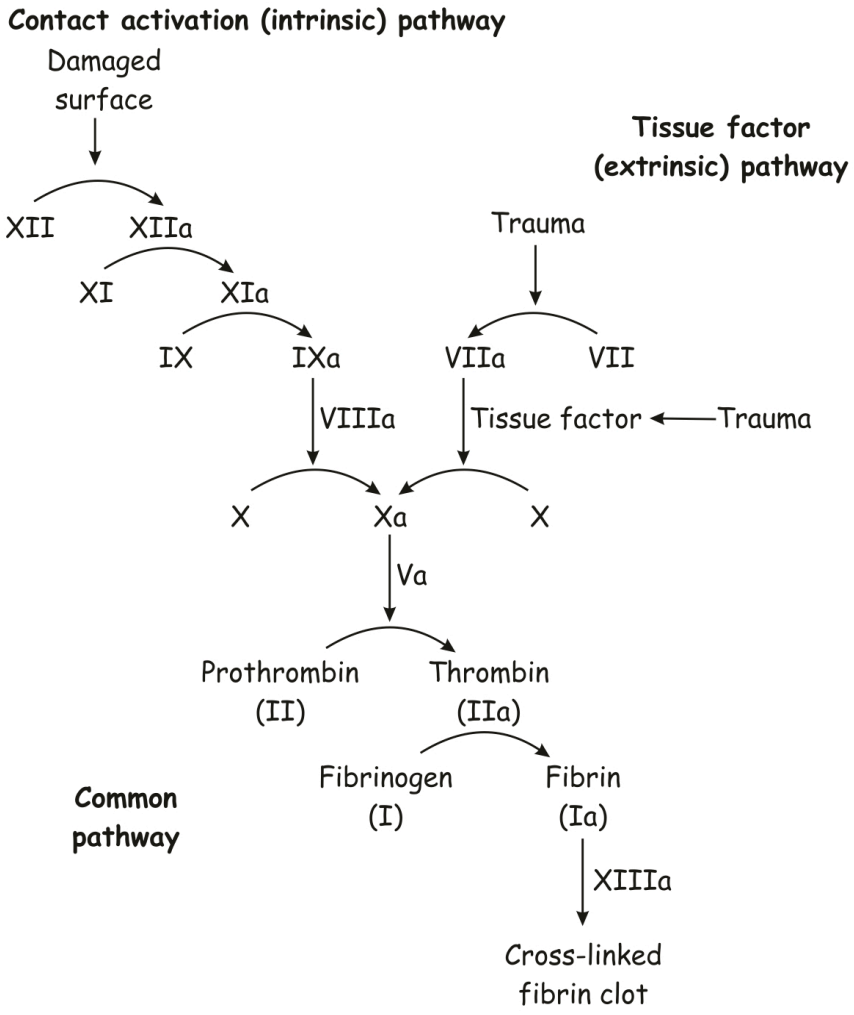

Figure 1.6 A resumptive scheme of the coagulation cascade, with the intrinsic and the extrinsic pathways. Gorbet, M. B., & Sefton, M. V. (2004). Biomaterial-associated thrombosis: roles of coagulation factors, complement, platelets and leukocytes. *Biomaterials, 25*(26), 5681-5703. Reproduced with permission.

The coagulation is a cascade of reactions, where an enzyme actives another enzyme until the transformation of the prothrombin to thrombin by factor Xa/Va. The first reactions that start the cascade are two: in the case of intrinsic pathway the coagulation is triggered by the contact of the blood with a foreign surface; for the extrinsic pathway it is triggered by the tissue factor (TF) produced by cells.

In the intrinsic pathway, the contact activation system of the blood involves various proteins at

the first stage. The most probable reaction that occurs is the zymogen activation of the Factor XII and the high molecular weight kininogen (HMWK) by the contact with a negatively charged surface that initiate a cascade of reactions (Colman, 1984). On the other hand, the extrinsic pathway occurs when the TF is expressed by damaged cells at the site of the vascular injury. At this point, activated Factor VII binds the TF, forming the so called extrinsic tenase complex that starts the coagulation cascade.

However, the two pathways are not independent, indeed the extrinsic pathway has a major role in the beginning of the coagulation, while the intrinsic pathway has a major role in propagation of the coagulation, in fact, it activates Factor X that is associated with clot formation (Rand, Lock, van't Veer, Gaffney, & Mann, 1996).

In the presence of a biomaterial, the activation of Factor XII, and so the intrinsic pathway, occurs because the biomaterial constitutes the necessary negatively charged surface. In addition, HMWK and kallikrein are adsorbed; initially fibrinogen is adsorbed and later is substituted by HMWK as described by Leo Vroman (Vroman, Adams, Fischer, & Munoz, 1980). However, some studies have demonstrated that when biomaterials are in contact with only plasma proteins, a little amount of thrombin is generated, suggesting that plasma proteins without platelets and leukocytes are not enough to start the coagulation cascade (van der Kamp, Hauch, Feijen, & Horbett, 1995).

1.3.2.5 Complement system

The complement system is a group of about twenty plasma proteins, enzymes and binding proteins that have an essential role in the body defense against infections and non-self elements.

There are three pathways that activate the complement system: classical, alternative and via lectin. In any case, the result is the generation of various proteins with different functions: opsonization, chemotaxis, cell lysis, elimination of the antigen-antibody complex, and activation of B-lymphocytes. Opsonization is the process that facilitates the phagocytosis of foreign materials and cells bound to the complement proteins. Chemotaxis is the process of attraction of leukocytes by chemical substances of the complement system (Andersson, 2003). The complement and the coagulation systems are highly interconnected and they are immediately

activated after any kind of vascular injury (Amara et al., 2008)

Traditionally, the behaviour of biomaterials has been classified as non-activating or activating of the complement system. Among non-activating surfaces, there are negatively charged surfaces, while in the activating surface category, there are nucleophiles rich surfaces and other ones that bind other complement proteins. Moreover, the complement activation doesn't depend only on the type of complement proteins adsorbed but also on the quantity of bound proteins that can disturb the complement system equilibrium.

1.3.2.6 Leukocytes

Leukocytes or white blood cells are cells of the inflammatory and immune systems involved in the defense of the body against foreign agents and materials. There are five types of leukocytes in the circulation: neutrophils, monocytes, lymphocytes, basophils and eosinophils. In the case of vascular devices, the major role of leukocytes in the inflammatory response is carried out by neutrophils and monocytes. Leukocytes have receptors for complement proteins, some platelet products and bacteria. It has been demonstrated that activated platelets secrete various products that interact with leukocytes and can influence the inflammatory response stimulating or inhibiting leukocytes (Klinger, 1997). In addition, platelets have an important role in the recruitment of leukocytes at the site vascular injury.

The activation of leukocytes produces some physiological changes in the cell. First of all, after activation, neutrophils and monocytes express different membrane receptors and proteins among which the TF that is involved in the coagulation process. Thereafter, leukocytes release granules containing inflammatory mediators that can activate platelets or other leukocytes, or promote their adhesion to the endothelium and other surfaces. In certain cases, neutrophils and monocytes release reactive oxygen species, starting the oxidative burst.

Leukocytes, in particular neutrophils and monocytes, are activated by their contact with artificial surfaces. This can occur directly, through complement system, or through activated platelets (Gawaz, Langer, & May, 2005). After the interaction with vascular grafts, leukocytes are subjected to a frustrated phagocytosis and subsequently they fuse together forming multinucleated giant cells and releasing proteolytic enzymes that contribute to the degradation of

the matrix or the foreign materials (Brown, Ratner, Goodman, Amar, & Badylak, 2012).

As discussed before, the formation of thrombus is a patho-physiological blood reaction that leads to the failure of small diameter vascular grafts. Given that platelets, in addition to their adhesion, activation, secretion and aggregation properties, are central to the coagulation process and to leukocyte activation and recruitment, the first area of intervention in order to reduce the thrombogenicity of vascular grafts should be directed to interfere with platelet function. Accordingly, synthetic vascular surfaces with adequate properties to reduce thrombogenicity are needed in order to decrease the unwanted and pathological reactions of platelets without affecting their healing promoting properties.

1.4 Problem identification

Nowadays, a successful small diameter vascular graft doesn't exist, even if many efforts have been made in order to achieve it. Any technological solution proposed has shown to be not appropriate because of the short-term hemocompatibility that is thrombogenicity. The general problem is to find a technological solution in order to avoid the thrombus formation at the implant of small diameter vascular grafts.

1.5 General objective

The general objective of this research is to develop a non-woven structure with electrospinning in PET and to verify its performance as structure for small diameter graft.

1.5.1 Specific objectives

The first specific objective is to study and develop several non-woven structures with different fibre diameters and fibre orientations.

The second objective is to test the thrombogenicity of the electrospun structures with different fibre orientation, studying the platelet adhesion with a qualitative essay that is fluorescent labelling of platelets.

The last objective is to select the less thrombogenic structure among the surfaces with different fibre diameter measuring the platelet adhesion with a quantitative essay that is radioactive labelling of platelets.

CHAPTER 2 MATERIALS AND METHODS

In this chapter, the materials and methods used for the electrospinning and the thrombogenicity tests will be presented. In particular, the electrospinning setup and conditions, how the images with scanning electron microscope and confocal microscope were taken, the perfusion system for the simulation of the fluid dynamics conditions in small calibre vessels, and the protocols for platelet labelling will be shown.

2.1 Electrospinning

2.1.1 Electrospinning setup and conditions

The electrospinning process has been carried out at Polytechnique Montréal. The homemade setup that has been assembled is shown in Figure 2.1. It is composed of the following elements:

- a high voltage supply (Gamma Inc.);
- a syringe pump to make the solution flow at constant rate (PHD 4400, Harvard Apparatus);
- a 5ml glass syringe with a stainless steel needle (Popper & Sons Inc.);
- a stainless cylindrical drum (10 cm diameter);
- a direct drive electrical motor to make the drum rotate (built at Chemical Department at Polytechnique Montréal).

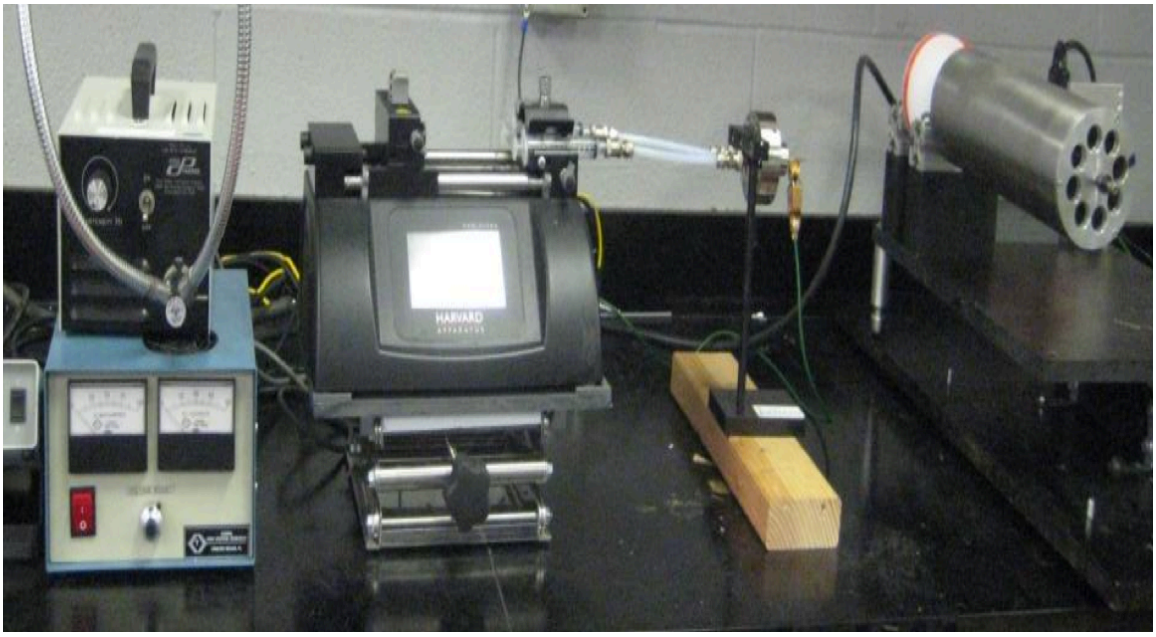

Figure 2.1 The homemade electrospinning setup at Polytechnique Montréal. From left to right: power generator, syringe pump to produce constant feedrate, syringe and needle touching one electrode (clamp with the green wire), grounded rotating collector mounted on its electrical motor.

PET with intrinsic viscosity of 1 (Selar PT7086) was obtained from DuPont, while PET with intrinsic viscosity 0.8 (Laser+ 7000 B92A) was obtained from DAK Americas.

The solvents that we used to make electrospinning solution were dichloromethane (DCM) and trifluoroacetic acid (TFA). Both were purchased at an analytical standard grade from Sigma Aldrich. The electrospinning solutions were obtained adding PET pellets in a TFA and DCM solution at the same relative concentration that is 1:1. After that, the final solution was stirred at low rounds per minute (rpm) for 24 hours in order to completely dissolve PET.

The weight per volume (w/v) concentration of PET in TFA/DCM solvent was calculated with the following equation:

$$PET\ concentration\ = \frac{PET\ mass}{TFA\ volume + DCM\ volume + \frac{PET\ mass}{PET\ density}} \qquad (2.1)$$

The value used for PET density is 1.33 g/cm^3 as calculated by Hadač et al (Hadač, Slobodian, & Sáha, 2007).

PET with intrinsic viscosity of 1 was dissolved in TFA/DCM (1:1) in various concentrations: 7.8 %, 8.1 %, 8.5 %, 9.0 %, 9.3 %, 11.4 %, 12.9 % (w/v). PET with intrinsic viscosity of 0.8 was used in solutions of 7.8 %, 9.3 % and 12.9 %.

Feed rate ranged from 0.2 to 1 mL\min, voltage from 10 to 30 kV, while the distance between tip and collector was fixed at 15 cm and the needle inner diameter was always the same at 22 gauge.

The collector was the same in every test, so the diameter was 10 cm, which means that the drum linear velocity depended only on the angular velocity of the collector. The angular velocity was set at 73, 365 and 438 rounds per minute corresponding to a linear velocity of 22.9 m/min, 114.7 m/min and 137.6 m/min, respectively. At 438 rpm the transmission belt broke down, settling the angular velocity upper limit at 365rpm.

The electrospinning conditions for the structures used in the experiments are presented in Table 2.1. The selection of the best conditions has been carried out in the following manner.

A selection of the polymer concentration in the electrospinning solutions was necessary because of their spinnability. The four polymer solution concentrations of 7.8 %, 9.3 %, 11.4 % and 12.9 % (w/v) were selected for the PET with intrinsic viscosity of 1, and the concentration of 7.8 % was chosen for the PET with intrinsic viscosity of 0.8.

For the process parameters, three feed rates were chosen: 0.2 mL/min, 0.5 mL/min and 1 mL/min. They were assigned in ascending order as the polymer concentration augmented in order to obtain structures with four different fibre diameter. At the beginning of the electrospinning process, the voltage was adapted in order to stabilize the electrospinning jet in a range between 14 kV and 25 kV.

Table 2.1 Electrospinning conditions for every surface selected.

STRUCTURE NAME	POLYMER SOLUTION			PROCESS CONDITIONS		COLLECTOR		AMBIENT PARAMETERS	
	PET intrinsic viscosity	PET concentration (w/v %) [g/mL]	Solvent	Voltage [kV]	Feedrate [mL/min]	Angular velocity [rpm]	Linear velocity [m/min]	Relative humidity [%]	Temperature [°C]
A1	1	7.8	TFA-DCM 1:1	19	0.2	73	22.9	8.5-10.5	23-25
A2	0.8	7.8	TFA-DCM 1:1	25	0.2	73	22.9	8.5-10.5	23-25
B1	1	9.3	TFA-DCM 1:1	18	0.5	73	22.9	8.5-10.5	23-25
B2	1	9.3	TFA-DCM 1:1	19	0.5	365	114.7	8.5-10.5	23-25
C1	1	12.9	TFA-DCM 1:1	15	1	73	22.9	8.5-10.5	23-25
C2	1	12.9	TFA-DCM 1:1	18	1	365	114.7	8.5-10.5	23-25
D1	1	11.4	TFA-DCM 1:1	14	1	73	22.9	8.5-10.5	23.25

2.1.2 Scanning electron microscope images

A scanning electron microscope (SEM, JEOL, JSM-6100) at a voltage of 15kV was used to take images at "Centre de Caractérisation Microscopique des Matériaux" $(CM)^2$ in Polytechnique Montreal. The electrospun structures were cut and mounted on SEM holders and a gold coating under vacuum was applied for 2 minutes. For every structure we took SEM images with three magnifications. Two of them, 500x and 2000x, were used to visually analyze the orientation of the nanofibers; the third magnification, 10000x for structures A1, A2, B1, B2, D1 and 4000x for structures C1 and C2, was used to calculate the fibre diameter using the image processing software ImageJ (National Institutes of Health, 2012). For every structure two samples and at least 50 fibres randomly chosen per sample were measured.

2.1.3 Porosity measurement

From each dry electrospun structure, two samples were cut. Width and length were measured with a digital caliper; thickness was measured with a high resolution thickness gauge (Film Master, Qualitest); and mass was measured with an electronic balance (AE100, Mettler Toledo).

The equation (2.1) was used in order to calculate the porosity of the electrospun non-woven structures (Hadjizadeh et al., 2011):

$$Porosity(\%) = \left(1 - \frac{PET\ apparent\ density}{PET\ bulk\ density}\right) \times 100 \qquad (2.1)$$

where PET apparent density is defined in equation (2.2) as:

$$PET\ apparent\ density = \frac{PET\ mat\ mass \times PET\ mat\ thickness}{PET\ mat\ area} \qquad (2.2)$$

The value used for PET bulk density was 1.33 g/cm^3 as calculated by Hadač et al (Hadač et al., 2007).

2.2 Thrombogenicity

2.2.1 Perfusion setup

The thrombogenicity tests were carried out at the Montreal Heart Institute. We used an experimental setup that mimics fluid dynamics of small diameter vessels (Badimon, Turitto, Rosemark, Badimon, & Fuster, 1987). The setup is showed in Figure 2.2 and it's composed of the following elements:

- peristaltic pump (Masterflex L/S 7518-10, Cole-Parmer Inc.);
- perfusion chambers with inner diameter of 2 mm;
- tubing (Tygon R-1000, Fisher scientific);
- heating system (Lauda).

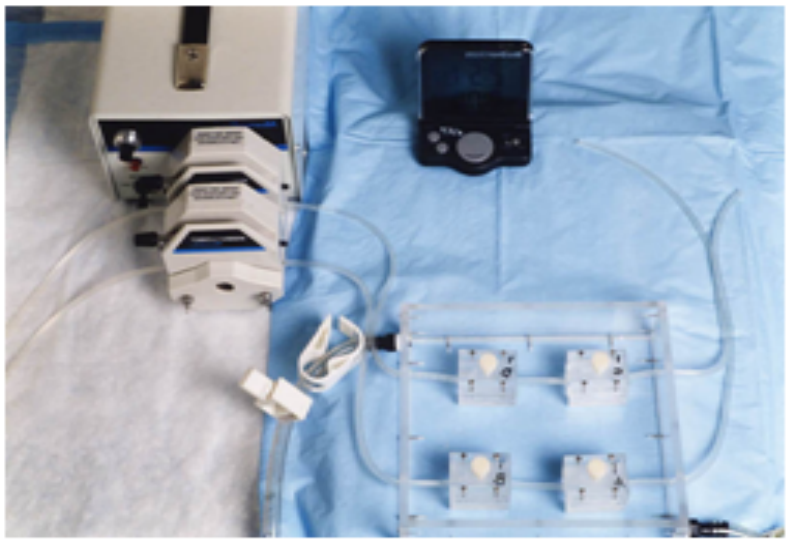

Figure 2.2 Experimental set up for thrombogenicity tests that mimics the fluid dynamics of small diameter vessels.

The perfusion chambers are shown in Figure 2.3. They are composed of a Plexiglas body with a cylindrical duct of inner diameter of 2 mm and 10 mm long in a rectangular chamber, which is closed by a plastic cap and tightened up to the body with a screw.

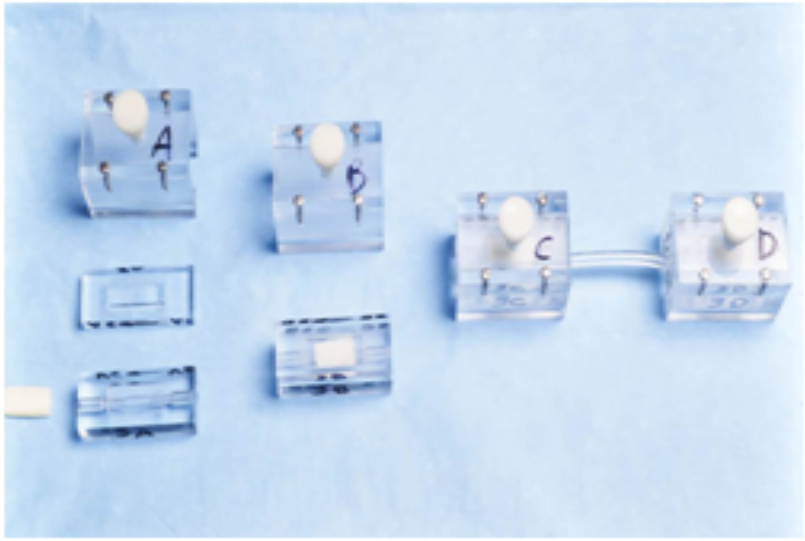

Figure 2.3 Perfusion chamber and its elements.

Every type of structure has been tested in duplicate with two sequential perfusion chambers per experiment. During the perfusion, chambers and blood were submerged by water at 37 °C in order to maintain the whole system at the biological temperature. Every perfusion lasted 15 min, which is enough time to let platelets be activated and adhere to the electrospun structure.

2.2.2 Shear rate and volumetric flow rate choice

The vessels that we want to simulate with the perfusion setup are small diameter vessels. For this reason, we chose an appropriate volumetric flow rate of blood in the perfusion chambers, so that the shear rate value in the duct simulates the conditions in small diameter vessels. In Figure 2.4 are presented *in vivo* observations of shear stress in biological vessels. The small diameter vessels we deal with have a dimension comprised between arterioles and conduit arteries, so we chose as referring value a shear rate of 800 sec^{-1} (Papaioannou & Stefanadis, 2005).

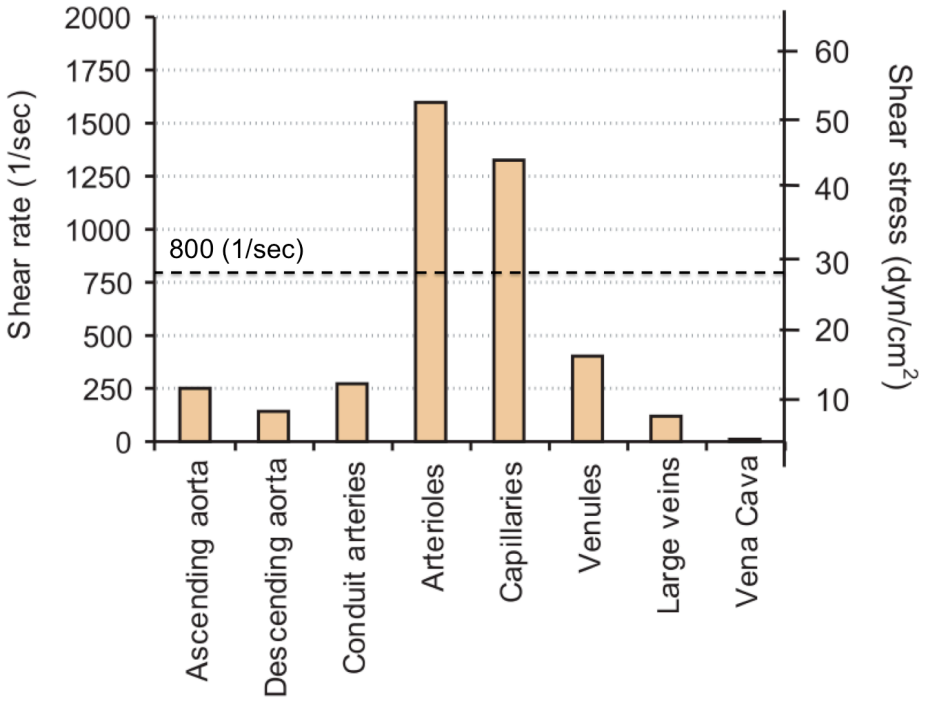

Figure 2.4 Shear stress and shear rate in various vessels. The small diameter vessels have a diameter and fluid dynamics between conduit arteries and arterioles. Adapted from "Papaioannou, T. G., & Stefanadis, C. (2005). Vascular wall shear stress: basic principles and methods. *Hellenic journal of cardiology : HJC = Hellenike kardiologike epitheorese, 46*(1), 9-15". Reproduced with permission.

The calculation of the volumetric flow rate that matches with biological shear rate have been done with two main approximations: blood has been considered a Newtonian fluid (Suh, 2007) and the perfusion chamber duct have been considered cylindrical (Merhi, King, & Guidoin, 1997). With these approximations we could use the Hagen-Poiseuille equation (2.3) (Paszkowiak & Dardik, 2003):

$$\tau = Q \times \frac{4 \times \mu}{\pi \times r_d^3} \qquad (2.3)$$

Where τ is shear stress [Pa], Q is volumetric flow rate [cm^3/s], μ is blood kinetic viscosity [Pa s], and r_d is the radius of the cylindrical duct [cm]. For a Newtonian fluid we can calculate the shear rate $\dot{\gamma}$ from shear stress and viscosity with the equation (2.4):

$$\dot{\gamma} = \frac{\tau}{\mu} \tag{2.4}$$

So, we calculated the volumetric flow rate from the equation (2.5):

$$Q = \dot{\gamma} \times \frac{\pi \times r_d^3}{4} \tag{2.5}$$

We considered the shear rate in order to simulate the small diameter vessels conditions of 800 sec^{-1} and the duct radius of 0.1 cm. The volumetric flow that corresponds to these calculations is about 0.63 cm^3/s (or 38 mL/min) (Merhi et al., 1997).

2.2.3 Electrospun surfaces sterilization

The electrospun non-woven structures were cut in a rectangular shape (2 cm x 1 cm) along the longitudinal direction in order to have a surface with constant thickness as presented in Figure 2.5.

For sterilization, the cut surfaces were placed in a 12-well plate, submerged for 5 minutes in 70% ethanol and rinsed out three times with distilled water. Finally, surfaces were placed in the perfusion chambers when completely dry.

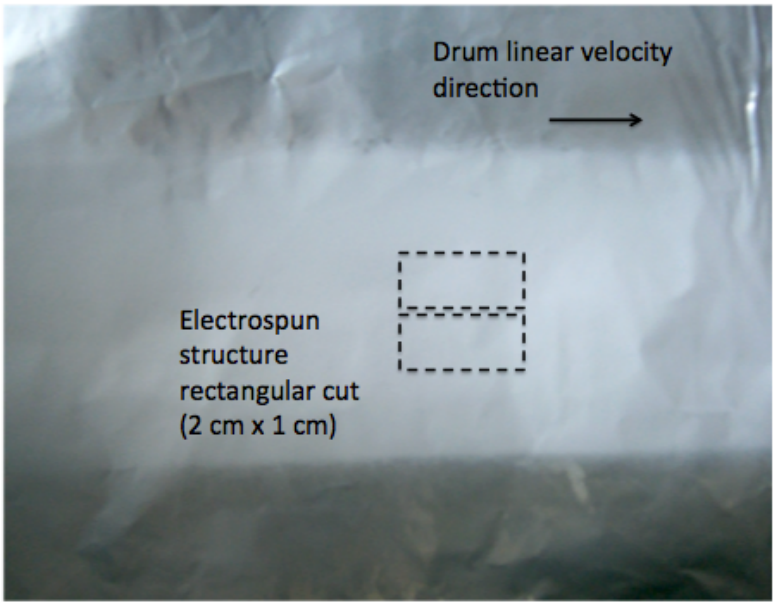

Figure 2.5 The electrospun nanofibrous non-woven structure (white deposition on the aluminum foil) was cut in a rectangular shape along the direction of the drum linear velocity in order to have a surface with constant thickness.

2.2.4 Rhodamine labelling of platelets

For the first thrombogenic essay, human platelets were labelled with a fluorescent molecule: rhodamine 6G (Sigma-Aldrich). First of all, fresh human blood from healthy donors was collected and D-phenylalanyl-L-prolyl-L-arginine chloromethyl ketone (PPACK) (Calbiochem) was used as anticoagulant. Afterwards, we prepared a suspension of rhodamine 6G and distilled water at concentration of 10 μg/mL; then, 50 μL of suspension was added to 10 mL of blood for a final concentration of 50 ng/mL of rhodamine 6G in the blood sample. The final suspension was incubated for 15 min at 37 °C.

The rhodamine 6G labelled blood was used in the perfusion system in contact with electrospun structures for 15 min with a volumetric flow rate of 38 mL/min. After blood perfusion, the system was emptied of blood, washed for 20 sec with saline solution (0.9% Sodium Chloride, B. Braun Inc.) and filled with 10% paraformaldehyde (Sigma-Aldrich) for 30 min for platelet fixation.

2.2.5 Confocal microscope images

After fixation of adherent platelets, the non-woven electrospun structures were prepared for fluorescent microscopy. The structures were removed from the perfusion chambers and placed on a microscope slide with the side in contact with blood upwards. Then, a solution of 1,4-diazabicyclo[2.2.2]octane 0.01% (DABCO) in glycerol was applied on the surface in order to improve the life time of rhodamine, and covered with a cover slip.

The confocal images were taken at the Montreal Heart Institute with a confocal microscope (LSM710, Zeiss) equipped with an objective (Plan-Achromat) 63x/1.4. For every surface tested, we took three types of images: single, z-stack, and tile. The single and z-stack images covered an area of 224μm x 224μm, while tile was composed of 5 x 2 single images on the same focus plane for a covered area of 1120μm x 448μm. Z-stack is a series of single images of the same area taken every 0.33 μm in depth for a total depth of 9.9-13.2μm (30-40 single images) that show the platelet penetration along the electrospun structure. From the z-stack, we built with the software ImageJ (National Institutes of Health, 2012) the maximum intensity projection image. The maximum projection image is created choosing for every pixel of the output image the maximum value meet by a hypothetic ray that cross all images of the stack at that particular pixel location.

The wavelength chosen for the excitation of rhodamine 6G was 543 nm with a He-Ne laser.

The calculation of the area of red in tile images of structures B1, B2 and C1, C2 were made with the software ImageJ analysing 3 tile images from 3 different experiments.

2.2.6 Radioactive labelling of platelets

For the quantitative thrombogenic essay, we used the radioactive isotope indium 111 (^{111}In) (Pharmalogique) to label human platelets. The ^{111}In has a half-life of 2.8 days. The labelling method starts with the platelet isolation (Diener et al., 2009). First of all, fresh human blood from healthy donors was collected in acid citrate-dextrose (Baxter), as an anticoagulant. The blood was subsequently centrifuged for 15 min at 1000 rpm to obtain the platelet rich plasma (PRP). Afterwards, 1 μg/mL prostaglandin E1 (PGE1) (Sigma-Aldrich) was added to the PRP before centrifugation at 2300 rpm, in order to obtain the platelet poor plasma (PPP). The platelet pellet

was resuspended in Hank's balanced salt solution (HBSS) citrated buffer, and the suspension incubated for 15 min with 250 μCi of ^{111}In, and then centrifuged at 2000 rpm in the presence of 0.5 μg/mL PGE1 for 10 min. The supernatant was removed and the platelet pellet was resuspended in PPP. Platelet suspension was then mixed with fresh blood of the same donor that was collected in PPACK.

The radioactive labelled blood was used in the perfusion system in contact with the electrospun structures for 15 min with a volumetric flow rate of 38 mL/min. After blood perfusion, the system was emptied of blood and washed with saline solution for 20 sec. The electrospun surfaces were finally removed from the chambers and fixed in a solution of 2.5% gluteraldehyde in the gamma counter tubes.

2.2.7 Platelet deposition count

The tubes that contain the different exposed surfaces were then placed in a gamma counter (Minaxi 5000, Packard Instruments), in order to measure the level of ^{111}In counts per minute (cpm) on each exposed surface. The radioactivity of reference blood samples was also measured (^{111}In cpm per ml of blood). The number of platelets per ml of blood was measured using an automated cell counter (Coulter AcT Diff, Beckman Coulter). Platelet deposition per mm^2 of area was then calculated with equation (2.6) (Merhi et al., 1997).

$$Platelet\ deposition = \frac{^{111}In\ cpm\ in\ exposed\ segment \times \frac{No.\ of\ platelets\ per\ mL\ of\ blood}{^{111}In\ cpm\ per\ mL\ of\ blood}}{Surface\ exposed\ to\ blood\ [mm^2]} \quad (2.6)$$

2.3 Statistics

In order to analyse the significance of the radioactive thrombogenicity tests, the relation between the platelet count and the fibre diameter of the electrospun non-woven structures was calculated.

The correlation coefficient between the two variables was calculated using the following equation:

$$r = \frac{\sum_{i=1}^{n}(x_i - \bar{x})(y_i - \bar{y})}{\sqrt{(\sum_{i=1}^{n}(x_i - \bar{x})^2)(\sum_{i=1}^{n}(y_i - \bar{y})^2)}} \quad (2.7)$$

Where x_i are the fibre diameter measurements and $\bar{x}$ is the mean of the diameter measurements; y_i are the platelet deposition measurements and $\bar{y}$ is the platelet deposition mean calculation.

The calculated correlation coefficient was compared with the *r* thresholds depending on the sample size *n* shown in Table 2.2.

Table 2.2 The two-sided thresholds at 5% of the correlation coefficient *r* as a function of the sample size *n*. Savard, P. (2011). *Bases du génie biomédical : notes de cours : cours GBM 6125*. Notes de cours, École Polytechnique de Montréal. Reproduced with permission.

n	**5%**	***n***	**5%**	***n***	**5%**
3	1.00	16	0.50	29	0.37
4	0.95	17	0.48	30	0.36
5	0.88	18	0.47	40	0.31
6	0.81	19	0.46	50	0.28
7	0.75	20	0.44	60	0.25
8	0.71	21	0.43	70	0.24
9	0.67	22	0.42	80	0.22
10	0.63	23	0.41	90	0.21
11	0.60	24	0.40	100	0.20
12	0.58	25	0.40	200	0.14
13	0.55	26	0.39	500	0.09
14	0.53	27	0.38	1000	0.06
15	0.51	28	0.37		

The null hypothesis is that the relation between the two variables is not linear, which corresponds to a correlation coefficient r = 0. The correlation coefficients shown in Table 2.2 are the thresholds over that the null hypothesis is refused with a significance of 0.05%. In our case, the correlation coefficient is 0.76 with a size of 22 samples; so the null hypothesis is refused because the coefficient is over 0.42 (Bland, 1995), confirming that the relation between platelet deposition and fibre diameter is linear.

CHAPTER 3 RESULTS AND DISCUSSION

In this chapter, the results and their discussion will be presented. Firstly, the electrospinning technique has been used in order to investigate the effects on the dimension and the alignment of the fibres of the polymer by changing the intrinsic viscosity, the concentration of the polymer in the electrospinning solution and the drum linear velocity. Secondly, the thrombogenicity of the structures was tested analysing the adhesion of the human platelets labelled with a fluorescent agent and a radioactive agent.

3.1 Electrospinning results

The aim of the research on the electrospinning technique was to obtain non-woven surfaces with three different fibre diameters and two different alignment degrees. The parameters that have been varied, in order to change the fibre diameter, were the intrinsic viscosity of the polymer, and the concentration of the polymer in the electrospun solution; while the parameter that has been changed for the alignment of the fibres is the drum linear velocity. The other parameters have been maintained constants in every experiment (needle diameter, temperature, humidity) or have been adjusted only in order to have a stable Taylor cone and a continuous electrospinning jet (feedrate, electric field, distance between needle and collector).

3.1.1 Effect of the intrinsic viscosity of the polymer

As explained before, the intrinsic viscosity of the polymer is an important parameter in the electrospinning process because it is known to modify the surface tension of the electrospun solution. For that reason, two polymers with different intrinsic viscosities were used in order to obtain smaller diameter fibres leaving the other electrospinning conditions unchanged. The two polymers that have been investigated have an intrinsic viscosity of 0.8 and 1. In this case the fibre orientation is not prevalent in any direction because the linear velocity of the drum was very low and insufficient to produce the alignment of the fibres.

Three magnifications of 500x, 2000x and 10000x of the electrospun non-woven surface called A1 obtained with the polymer with intrinsic viscosity 1 are shown in Figure 3.1 A, B and C.
In Figure 3.1 A, two isolated spheres with a diameter of about 5 μm are present on the surface A1; their features that make us think that are two impurities, probably powder spheres, trapped in the surface during the electrospinning process. Looking at Figure 3.1 B, the fibres seem linear, without a prevalent alignment, as it was expected from the electrospinning conditions that have been chosen, and they are well separated one from each other, so it can be inferred that the time of flight of the jet is enough to let the solvent evaporate.
The calculation of fibre diameter and the porosity of structure A1 is presented in Table 3.1.

Table 3.1 Mean and standard deviation of fibre diameter, surface porosity and structure thickness of the electrospun selected structures.

Structure name	A1	A2	B1	B2	C1	C2	D1
Fibre diameter	259.3 ± 76.4 nm	234.0 ± 79.9 nm	388.1 ± 97.8 nm	374.4 ± 100.0 nm	1148 ± 446 nm	1314 ± 548 nm	429.2 ± 205 nm
Surface porosity	85.0 ± 2.0	85.0 ± 2.0	85.0 ± 2.0	85.0 ± 2.0	85.0 ± 2.0	85.0 ± 2.0	85.0 ± 2.0
Structure thickness	102 ± 7.0 μm	127 ± 6.2 μm	91 ± 5.8 μm	81 ± 3.1 μm	160 ± 5.5 μm	119 ± 7.0 μm	81 ± 6.5 μm

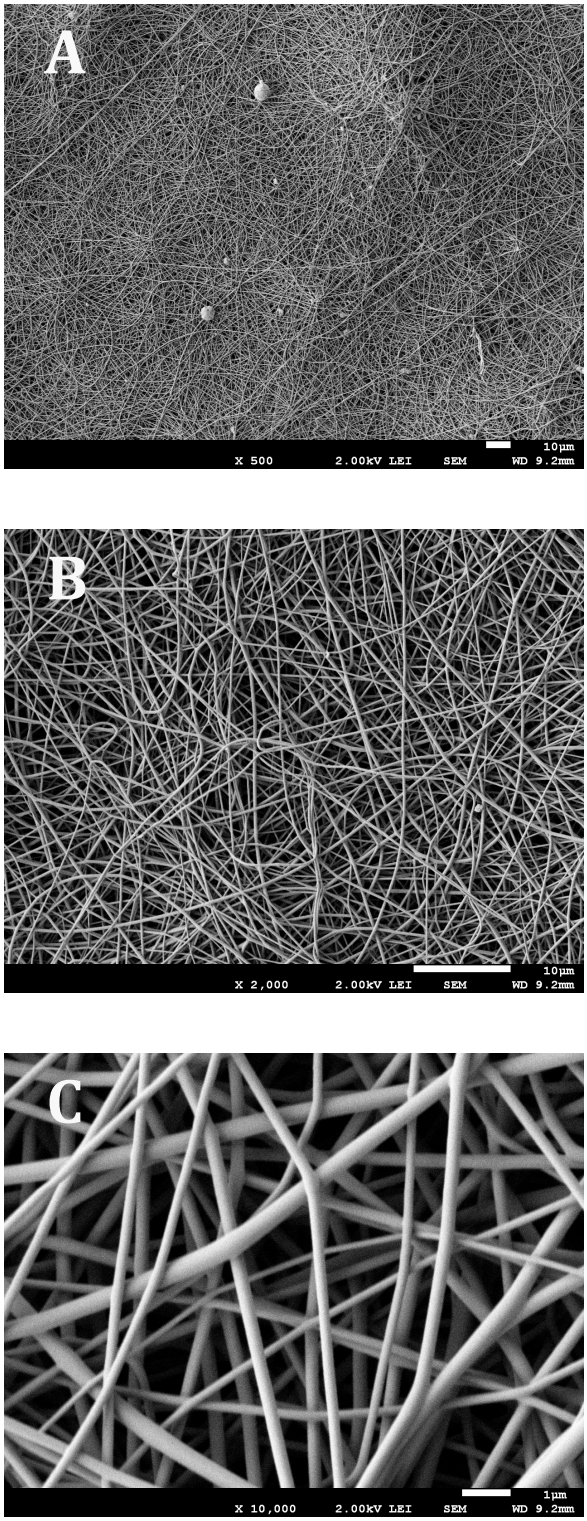

Figure 3.1 SEM images of the structure A1 with three magnifications A: 500x B: 2000x C: 10000x.

In Figure 3.2 A, B and C, three magnifications 500x, 2000x and 10000x of the non-woven surface called A2 are presented. The polymer that has been used has an intrinsic viscosity of 0.8. As seen in Figure 3.1 A, there is the presence of some spheres in the structure that probably are impurities incorporated during the electrospinning process. Indeed, in Figure 3.2 B it can be seen a magnification of the spheres, and it can be observed that they are not part of the fibres, but they are trapped in the non-woven structure as external corps; this fact excludes the possibility that they are beads in the fibres, that may originate from the instability of the electrospinning process.

In Table 3.1 the diameter of the fibres and the porosity of the structure is presented. The structures A1 and A2 result in a different fibre diameter (Table 3.1). The different intrinsic viscosity of the polymers that compose the structures A1 and A2 can explain this difference. As a matter of fact, when the intrinsic viscosity decreases without modifying the other electrospinning conditions, the viscosity of the solution also decreases. The surface tension is a force opposed to the electric forces that stretch the electrospinning jet; for that reason the electrospinning jet of the polymer with a lower intrinsic viscosity gives less resistance against the electrical stretching of the jet, resulting in smaller diameter fibres.

The difference in diameter between the two fibres of the structures A1 and A2 is about 25 nm, which is quantitatively insufficient to represent two structures with two different morphologies. In addition the structure A2 has more impurities than the structure A1. For those reasons, the structure A1 has been considered representative as a structure composed by small diameter fibres and it was chosen for the thrombogenicity tests.

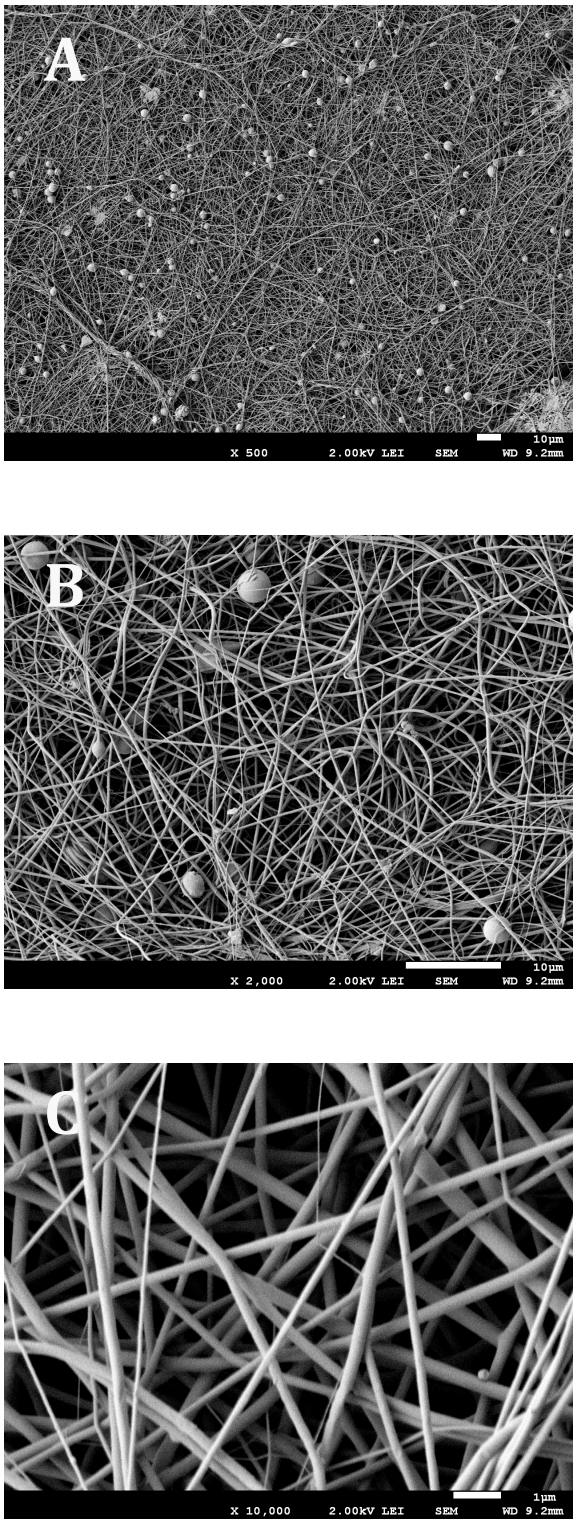

Figure 3.2 SEM images of the structure A2 with three magnifications A: 500x B: 2000x C: 10000x.

3.1.2 Effect of the drum linear velocity on the fibre orientation

The electrospinning consists in the deposition of a jet of solution on a collector. The collector and its movements permit to create a pattern of the electrospun fibres, originating a structure with particular morphology. In this research a circular collector has been used, and depending on its rotation velocity, oriented fibres could be produced.

In Figure 3.3 the SEM images of the electrospun structures obtained from a polymer with intrinsic viscosity of 1 as the structure A1 and polymer concentration higher than for the previous structures are presented. Because of the different conditions from structure A1, it was expected to obtain larger diameter fibres. In Figure 3.3 A, B and C, there are three magnifications (500x, 2000x and 10000x) of the structure B1. In this case, the drum linear velocity is the same as for structure A1, so the hypothesis that no fibre orientation should be remarked was made. Looking at the SEM images can be noticed that the surface has little impurities. In this case, the shape is not perfectly round, so the elongated spheres are beads formed during the process. The formation of occasional beads can happen also when the electrospinning jet is stable, because the drum linear velocity is not perfectly uniform and small air bubbles can be found in the solution. The first effect is due to the train of gears moved by the electric motor combined with the inertial forces of the rotation of the drum; while the second effect can occur because the viscosity of the solution makes difficult its suction into the syringe.

The fibre diameter and porosity of the structure B1 are showed in Table 3.1. As it can be seen, the fibre diameter is bigger than structure A1 and A2. The results agree with the predictions, because increasing the polymer concentration in the electrospinning solution produces more entanglements between the polymer chains, which augment the viscosity, and as consequence the nanofibre diameter.

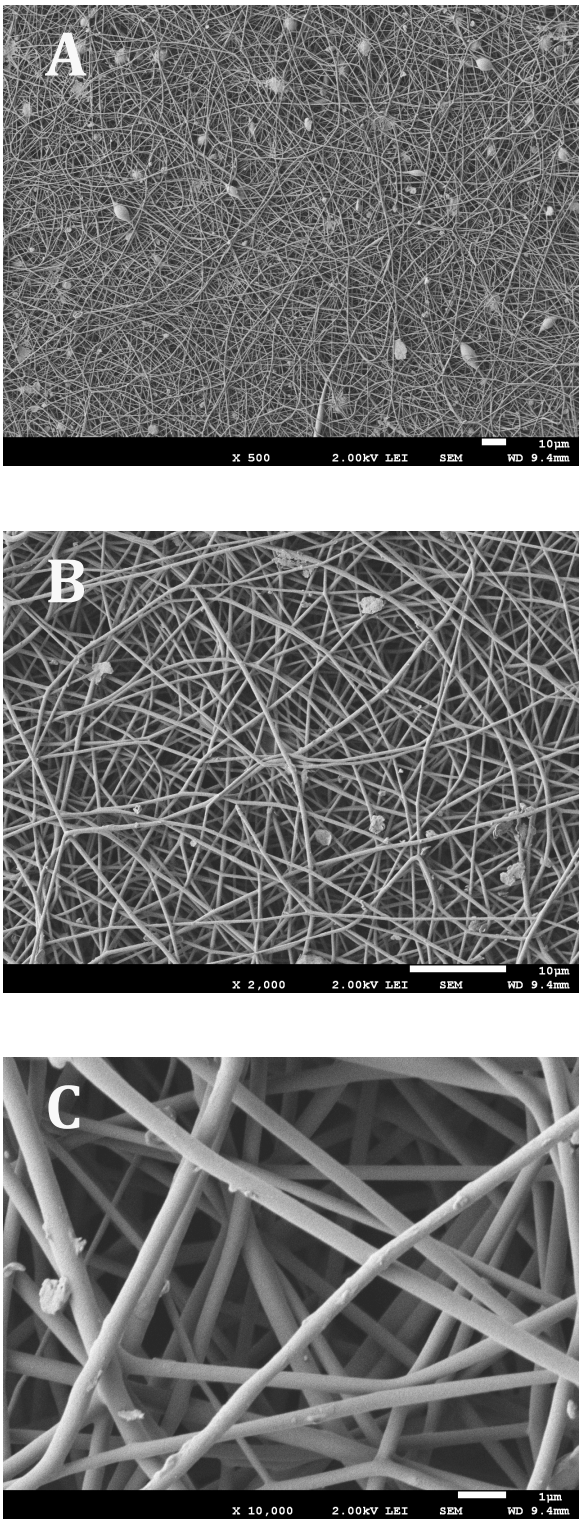

Figure 3.3 SEM images of the electrospun structure called B1 with three magnifications A: 500x B: 2000x C: 10000x.

The images of the structure B2 in three magnifications (500x, 2000x and 10000x) are shown in Figure 3.4 A, B and C. Structure B2 was obtained with the same electrospinning conditions as for structure B1 except for the drum velocity. The drum linear velocity is 5 times the drum velocity used for structure B1. For that reason, it was made the hypotheses that the fibres of structure B2 should have a prevalent orientation in the direction of the drum rotation compared to the fibres of structure B1.

In Figure 3.4 A, the presence in structure B2 of some beads and impurities can also be noticed. As explained for structure B1, some occasional beads can be produced during the electrospinning process caused by the electrical motor or air bubbles in the syringe. Furthermore, the presence of some impurities caused by powder particles trapped in the structure can be remarked.

Looking at Figure 3.4 A and comparing it with Figure 3.3 A, not evident difference in the orientation of the fibres can be remarked. The drum linear velocity seems to be not high enough to produce a significant alignment of the fibres.

The results on fibre diameter porosity of the structure B2 are presented in Table 3.1. As we expected, the fibre diameter of structure B2 is comparable with the fibres of structure B1; as a matter of fact the electrospinning conditions were maintained the same in both experiments. As it was expected, the changing of the collector linear velocity didn’t affect the fibre diameter.

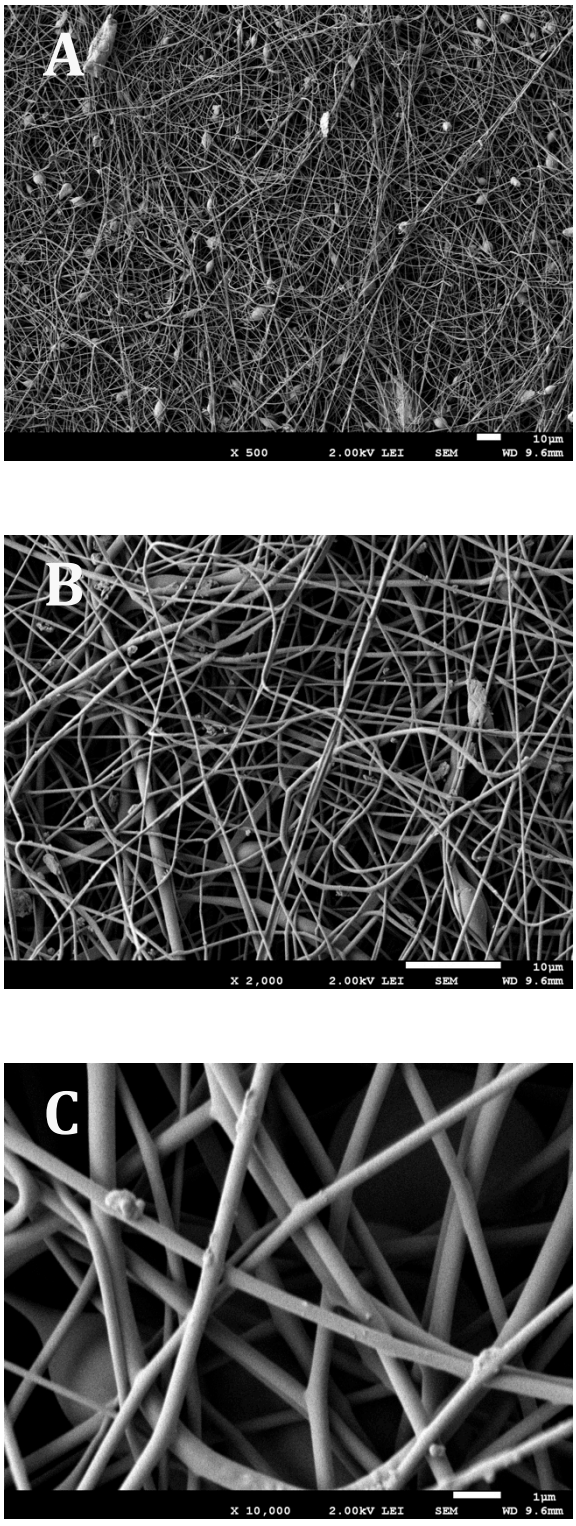

Figure 3.4 SEM images of the electrospun structure called B2 with three magnifications A: 500x B: 2000x C: 10000x.

Three magnifications of 500x, 2000x and 4000x of the structure C1 are showed in Figure 3.5. Compared to the previous structures, the structures C1 and C2 were obtained with a higher polymer concentration in the electrospinning solution and a higher feed rate. The other process parameters have been changed as little as possible in order to stabilize the electrospinning jet. The structure C1 has been obtained with a low drum velocity, so no fibre orientation was expected.

In Figure 3.5 A can be noticed that some fibres are beaded. The beads are smaller and more stretched than structures B1 and B2. We can explain their presence because the higher feedrate condition can produce a temporary Taylor cone instability resulting in the occasional formation of beaded fibres.

Looking at Figure 3.5, there is no evident orientation of the fibres.

The fibre diameter calculation results for the structure C1 are presented in Table 3.1. The fibres obtained are larger than the fibres of the previous structures; in fact the polymer concentration was higher. As a matter of fact, Figure 3.5 C has a magnification of 4000x, less than the corresponding images of structures A1 and A2, B1 and B2.

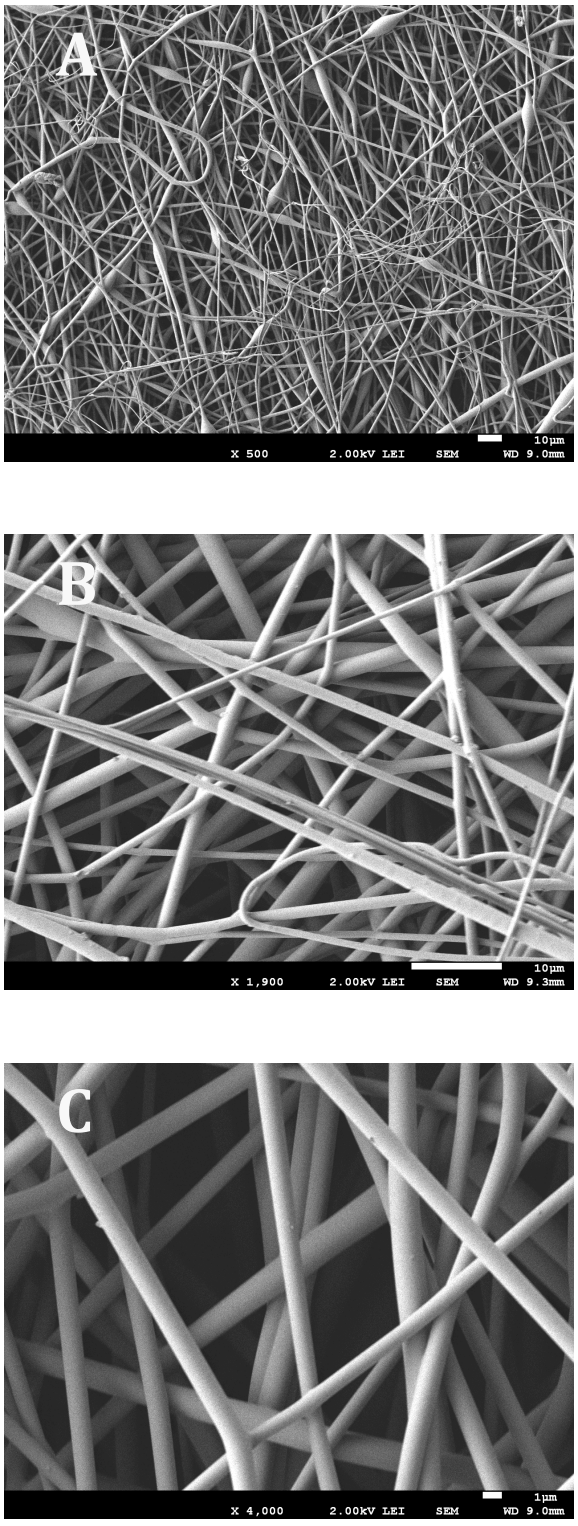

Figure 3.5 SEM images of the structure C1 with three magnifications A: 500x B: 2000x C: 4000x.

In Figure 3.6 A, B and C, are presented three magnifications (500x, 2000x and 4000x) of the structure C2. The parameters that were used to obtain this structure were the same as for structure C1 except for the drum linear velocity that was 5 times the previous one. It was expected to see a different orientation of the fibres like the structures B1 and B2, as the drum velocity is higher. In Figure 3.6 A the fibres that compose the structure are linear, without beads and other impurities. No prevalent orientation of the fibres was remarked, as they are not pointed in any prevalent direction.

The diameter of the fibres that is showed in Table 3.1 is comparable to the diameter of structure C2. At the same time, the fibre diameter of structures B1 and B2 is comparable; so it's confirmed that the electrospinning experiments are reproducible.

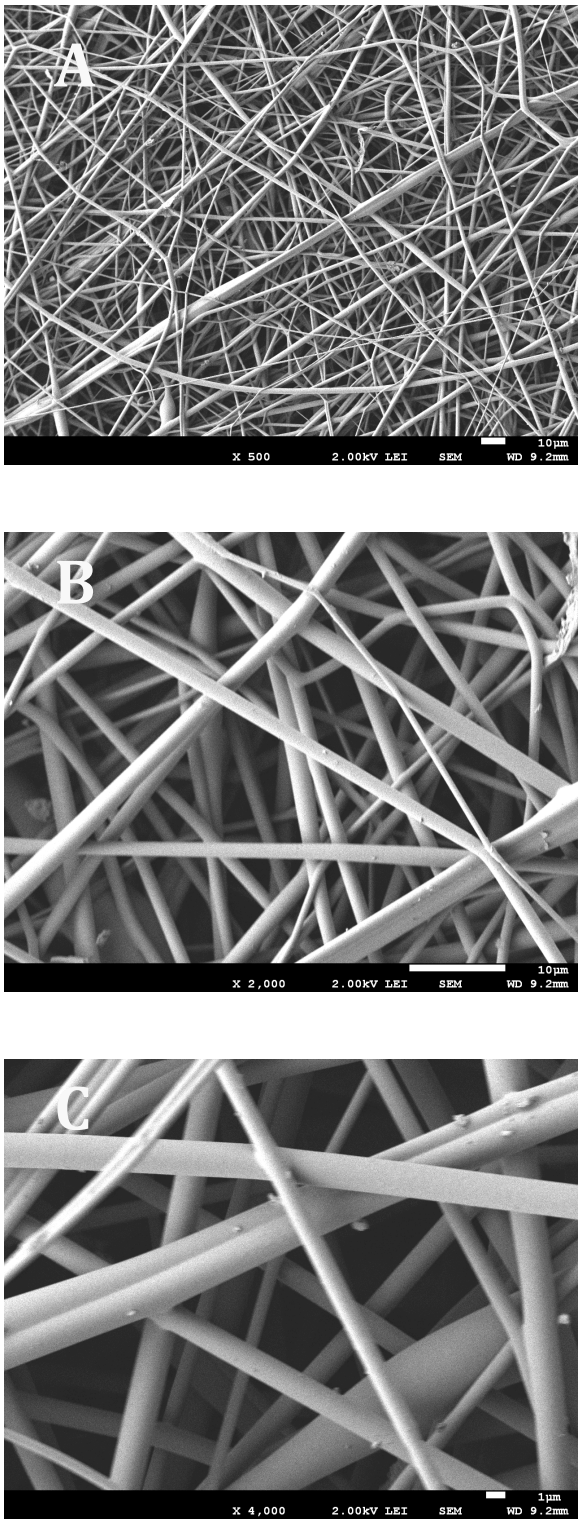

Figure 3.6 SEM images of the structure C2 with three magnifications A: 500x B: 2000x C: 4000x.

3.2 Thrombogenicity assay with rhodamine labelling

The fluorescent labelling is a qualitative technique to analyse platelet adhesion. In order to have a quantification of the area occupied by platelets, the surface coloured in red has been calculated. Nevertheless, because of the rhodamine labelling technique, the whole blood contains rhodamine, so PET fibres have been bonded by rhodamine and were stained of red. For that reason, the comparison of the area of red in confocal images can be done only between electrospun structures composed of fibres with the same diameter, so that the fibre staining contribution is the same.

With this technique, the platelet behaviour for structures with supposed fibre prevalent orientation was compared. Therefore, structures B1 and B2, and structures C1 and C2 have been obtained with two patterning conditions: aligned and not-aligned, so they were tested two by two with fluorescent thrombogenicity tests.

3.2.1 Thrombogenic behaviour of structures B1 and B2

Table 3.2 shows the area of red calculation for structures B1 and B2. The area of red appears to be higher for structure B2, in comparison with structure B1; however, the difference is not statistically significant. Furthermore, this calculation has two main limits. The first one is that the rhodamine was not always perfectly dissolved, so some rhodamine residues can remain trapped at the electrospun surface producing artefacts that vitiate the calculation; secondly, it has to be taken into account that tile images are series of single images taken at the same focus plan, so the irregularities of the electrospun surfaces can produce some dark not-focused areas that influence the result.

Table 3.2 The area of red calculation for structures B1 and B2, made from 4 tile images of different experiments per structure.

STRUCTURE	B1	B2
AREA OF RED	22.4 ± 6.1%	30.3 ± 5.7%

Figure 3.7 shows two representative tile images of structures B1 and B2. Figure 3.8 presents the maximum intensity projections, obtained as described in paragraph 2.2.5, of a portion of surface exposed to blood flow. The magnification of the images in Figure 3.7 and Figure 3.8 is the same, but the first ones were resized in order to fit the page.

Both images of Figure 3.7 present a red background composed of the nanofiber net coloured by rhodamine. The image of structure B1 presents some platelet aggregates of round shape coloured in red, but not homogenously distributed. The dimension of the red spots is not homogenous either; as a matter of fact, a bigger aggregate is present on the right side of the image. In the image of structure B2, the nanofiber net is more evident. Platelet aggregates are smaller than structure B1, but distributed homogenously. The left side of the image presents a dark spot caused by the wavy electrospun surface.

The different dimension of the aggregates suggests a different behaviour of platelets when got in contact with structures B1 and B2. Comparing the two structures, surface B2 seems to be more suitable for platelet adhesion than surface B1. In fact, platelet aggregates are integrated in the pores of B2, whereas in surface B1, the nanofiber net is less evident because the focus plane of confocal microscope was placed in an upper position in order to better focus platelets. In addition, the distribution of platelet aggregates in structures B1 and B2 is different. The surface B2 has a more homogenous distribution of platelet aggregates, which confirms that the nanofiber net facilitates platelet adhesion.

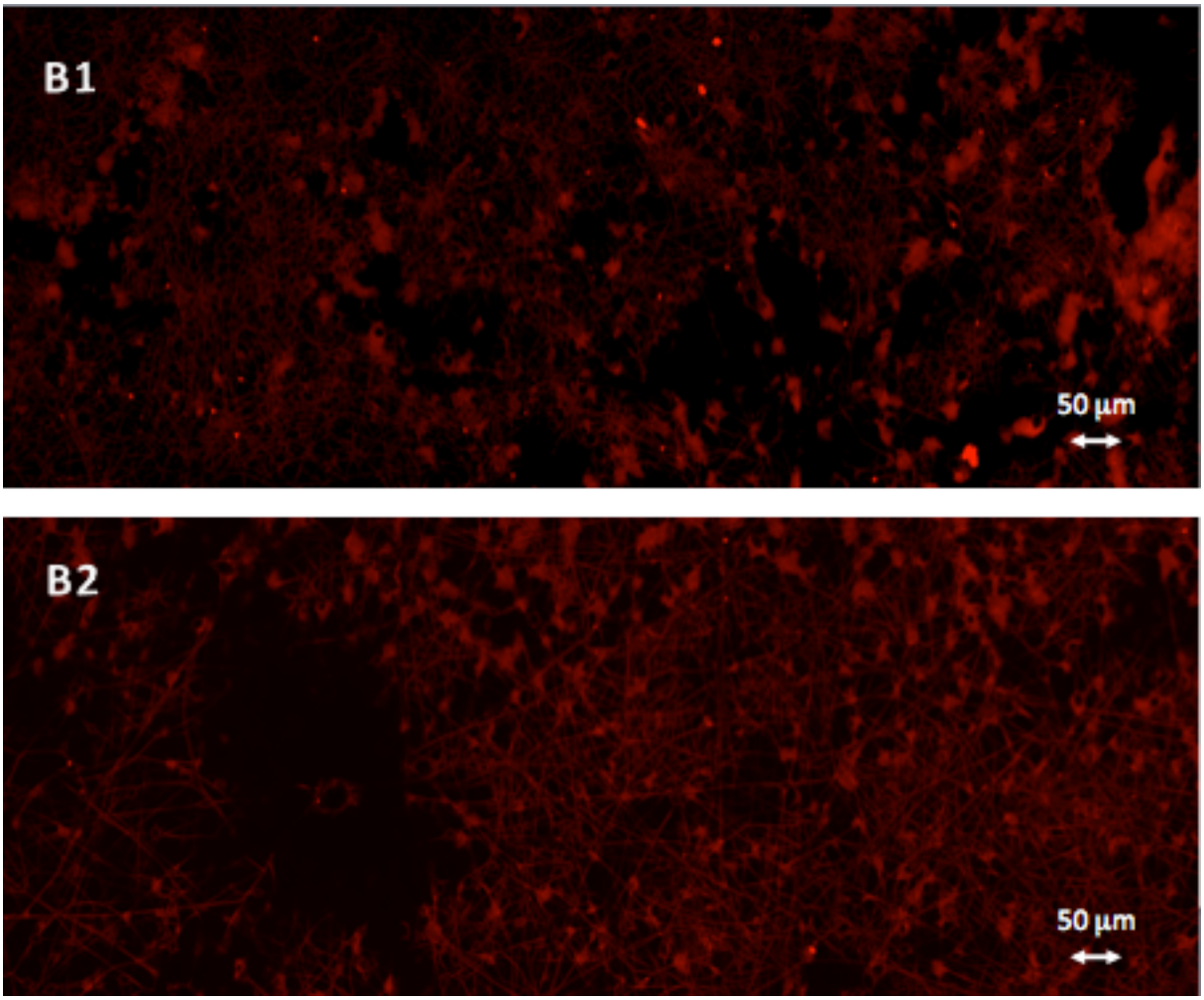

Figure 3.7 Tile images taken with confocal microscope of the structures B1 and B2 after the dynamic perfusion with rhodamine labelled blood. In both images we can see a background of stained red fibres with red spots generated by platelet aggregates.

Figure 3.8 shows a maximum intensity projection for structures B1 and B2. Z-stacks have the same magnification of the tile images, but cover an area ten times smaller than tile images. On the other hand, the maximum projection images are obtained from a series of images at different depth. For that reason, a z-stack is not enough to represent the whole surface behaviour, but gives punctual information on platelet connections with the nanofiber net.

In Figure 3.8, both structures B1 and B2 show a red background caused by the presence of the nanofiber net, but some platelet aggregates are evident in both structures. Platelet aggregates are different in the two structures: at surface B1, platelets are bound together in big aggregates, while

at the surface of structure B2, the aggregates are smaller and a lot of single platelets are visible near the nanofibers.

The presence of small aggregates and single platelets at the surface B2 confirms the homogenous distribution of platelets remarked in Figure 3.7. Therefore, even if at a visual analysis of the SEM images of structures B1 and B2 the fibre orientation was not evident, it probably has an effect on the thrombogenicity of the surface; structure B2 has a more thrombogenic potential than structure B1 and, for that reason, it was excluded in the following radioactive tests on the thrombogenicity.

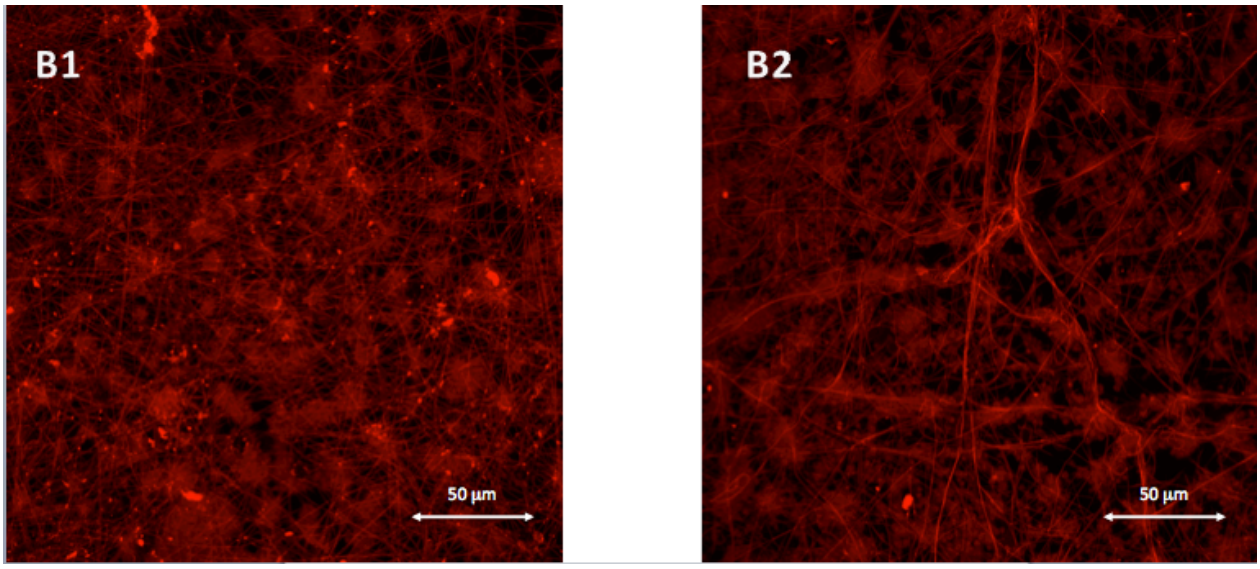

Figure 3.8 Maximum intensity projections of z-stack images of structures B1 and B2 for a representative portion of electrospun surface that come in contact with blood.

3.2.2 Thrombogenic behaviour of structures C1 and C2

Table 3.3 shows the calculation of the area of red for structures C1 and C2. In this case, the means are very similar and the slight difference is not statistically significant. As explained for structures B1 and B2, this calculation has limits due to the rhodamine artefacts and to the electrospun surface irregularities.

Table 3.3 The area of red calculation for structures C1 and C2, made from 4 tile images of different experiments per structure.

STRUCTURE	C1	C2
AREA OF RED	20.0 % ± 3.9	18.0 % ± 7.0

Two representative tile images of structures C1 and C2 are presented in Figure 3.9. The diameter of the fibres that compose structures C1 and C2 is bigger than structures B1 and B2. In that case, the fibre net is not clear, but can be noticed especially in the image of structure C2 due to the black lines. In fact, the inner part of the fibres was not stained by rhodamine.

Platelet aggregates on the two structures are different. The image C1 presents a low number of aggregates, concentrated in specific areas of the image. Furthermore, the fibre net is not evident and there are many dark spaces in the figure. The image of structure C2 shows a fibre net composed of black lines that interrupt platelet aggregates that are displayed as red spots. Platelet aggregates in structure C2 are small and uniformly distributed over the surface and around the fibres.

Comparing the two images, some considerations about the different behaviour of platelets can be made. First of all, platelet aggregates are smaller but more homogenously distributed on structure C2 than structure C1. This fact suggests that the fibre net of structure C2 favours platelet adhesion. Furthermore, the fibre net is more evident in the image of structure C2, because the focus plan of the confocal microscope was positioned at a lower plan than the image of structure C1. It can be deduced that platelets found a surface patterning more suitable for their adhesion and penetration in structure C2.

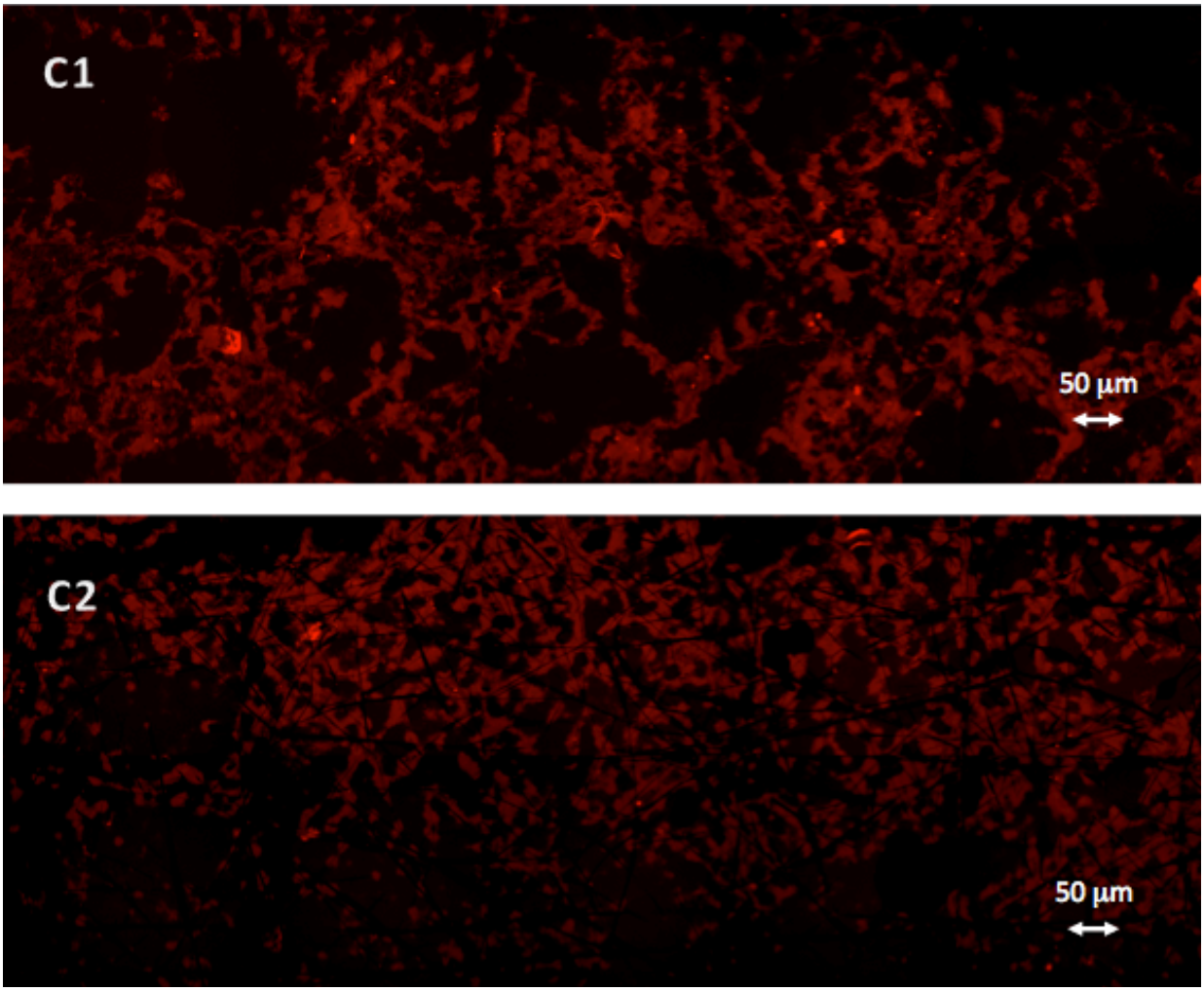

Figure 3.9 Representative tile images taken with confocal microscope of the structures C1 and C2 after dynamic perfusion with rhodamine labelled blood.

Figure 3.10 shows the maximum intensity projections of structures C1 and C2. In the image of structure C1, the fibre net can be noticed as black fibres that cross platelet aggregates, while in the image of structure C2, the aggregates are smaller and the fibre net is less evident. Furthermore, in the maximum intensity projection of structure C2, some single platelets that adhere to the fibres are present and there is a more uniform distribution of platelets on the surface.

The dimension of the aggregates and their uniform distribution in structure C2 indicate that the fibre orientation favours platelet adhesion on the whole surface. As noted for structures B1 and

B2, visual analysis of the SEM images didn't show any prevalent fibre orientation; but taking into account the confocal images of Figure 3.9 and Figure 3.10, we can infer that structure C2 is more thrombogenic. For that reason, the electrospun surface C1 was chosen for further investigations.

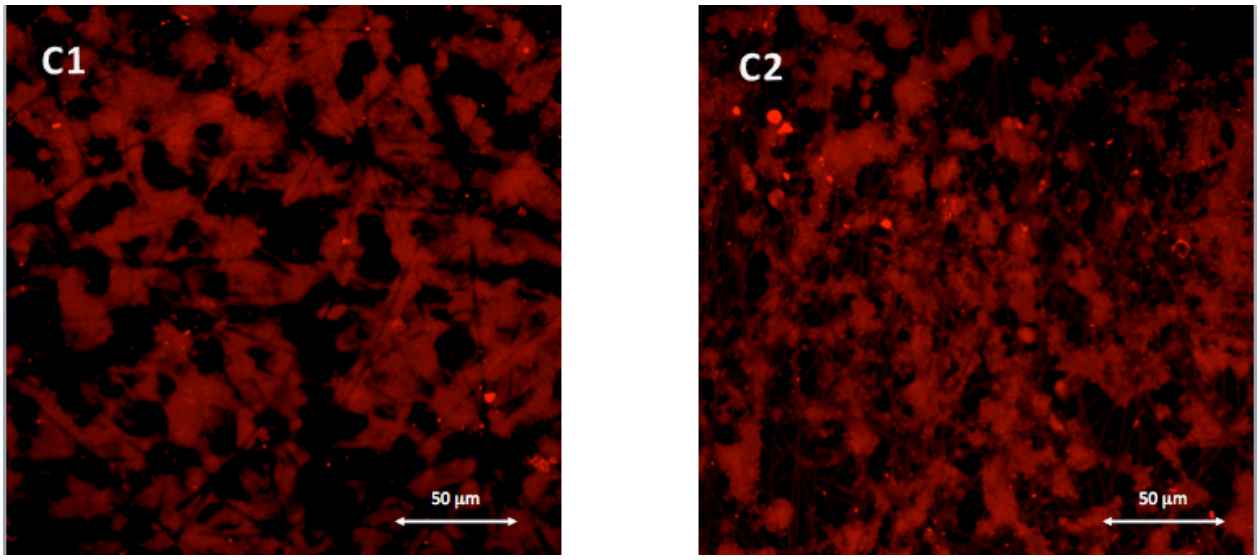

Figure 3.10 Maximum intensity projections of z-stack images of structures C1 and C2 for a representative portion of electrospun surface that come in contact with blood.

3.3 Thrombogenicity assay with radioactive labelling

The thrombogenicity of the electrospun surfaces A1, B1 and C1 was investigated in biological conditions with a perfusion system. Platelets were labelled with ^{111}In and mixed to fresh blood and their adhesion was tested under physiological fluid dynamics conditions. The surface of arteries with intact endothelium and tunica media (denuded artery) were used as positive and negative controls, respectively. The structures A1, B1 and C1 differ only in the diameter of the fibres that compose the non-woven structures. The other patterns and electrospun structures were excluded, as explained in the previous sections.

Figure 3.11 shows the results of platelet deposition on the different tested surfaces. The highest platelet adhesion with about 5500 platelets per mm^2 was seen on structure C1 that is composed of

fibres with the biggest diameter. Structure C1 induced a level of platelet adhesion that was statistically similar to the adhesion on the tunica media, used as positive control or thrombogenic surface, which had a mean deposition of 4800 platelets per mm^2. The structures B1 and A1 had a minor platelet adhesion, which is 2.5 and 6 times lower than structure C1, respectively. Finally, the endothelium, used as negative control or thromboresistant surface, was the less thrombogenic surface with a very low level of 450 platelets per mm^2. We noted that platelet adhesion on the different surfaces occurred with high variability between the experiments that resulted in high standard deviations. The experiments were carried out in different times, so fresh blood from different donors was used. Every donor ensured that he didn't take any drug that could interfere with the normal function of platelets; however, the number of platelets and their reactivity are different among donors, which may explain such variability in the results of platelet adhesion. In addition, the low number of experiments in this experimental setup contributed to such variations in standard deviations. Accordingly, the number of experiments should be increased in further investigations.

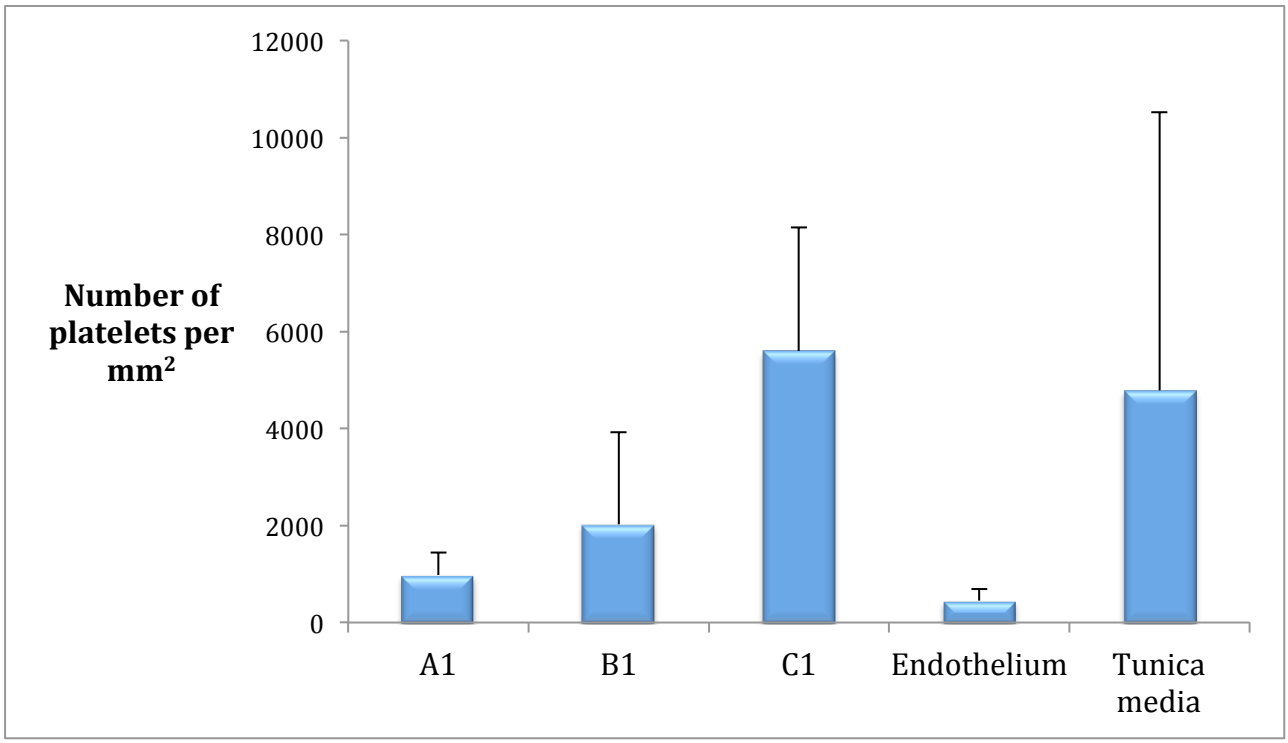

Figure 3.11. Platelet adhesion on the selected surfaces and on the endothelium and tunica media controls. The relation between the fibre diameter (structures C1, B1 and A1) and the platelet

adhesion is linear. It has been carried out 4 duplicate experiments for structures A1 and C1, 3 for B1 structure, endothelium and tunica media.

In order to relate platelet adhesion with changes in the fibre diameter, we analysed the correlation between them. In this analysis, we combined the results of fibre diameter (Table 3.1) and correlated them with those of platelet adhesion (Figure 3.11). A linear regression graphic was obtained, as shown in Figure 3.12. We can see that the relation between platelet adhesion and fibre diameter is significant, since the correlation coefficient between them is 0.76. We can conclude that platelet adhesion is influenced and related to the fibre diameter of the electrospun structures. In particular, the thrombogenicity of the structures decreases linearly with the diminution in fibre diameter.

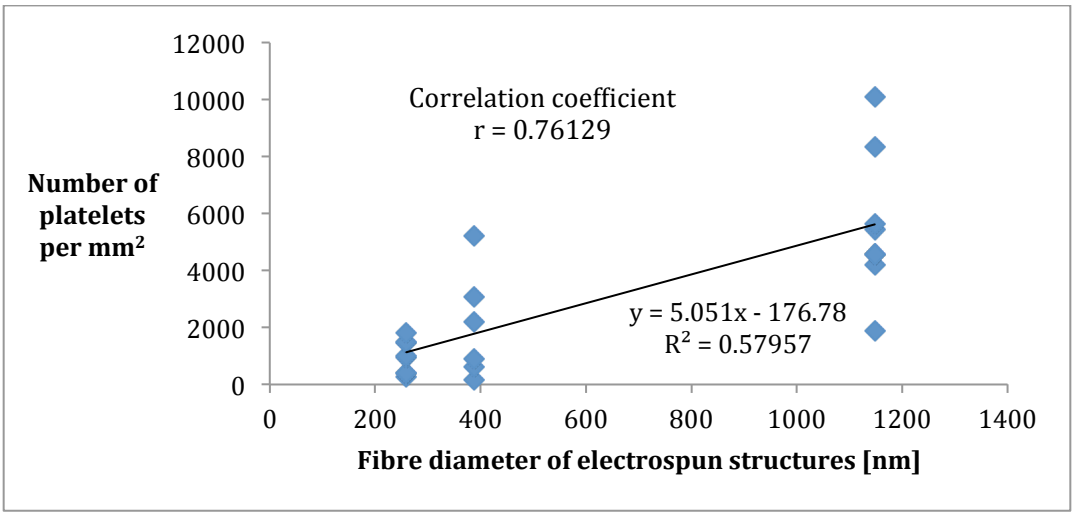

Figure 3.12 Linear regression graphic of platelet count on structures A1 (259 nm), B1 (388 nm) and C1 (1148 nm) as a function of the fibre diameter. The relation between number of platelets and fibre diameter is linear.

Given that our experimental conditions simulated the biological conditions found in small diameter vessels, we can infer that structure A1, among the tested artificial surfaces, has the best performance in term of thrombogenicity, which is close to that of intact artery with functional endothelium.

CONCLUSION

The electrospun nanofibrous PET structures have a great potential in biomedical applications. In particular, it is believed that they have a high potential as vascular prosthesis due to their mechanical properties and the pore features of non-woven nanofibers as scaffold for endothelial cells. Nevertheless, the thrombogenicity of the synthetic grafts limits their application as small calibre vessel substitutes.

In this dissertation, electrospun non-woven structures with various diameters and fibre orientations have been produced. The diameter of the fibres that compose the structures can be directly related to the polymer concentration in the electrospinning solution and to the feedrate of the solution. In particular, the decrease of the polymer concentration and the feedrate produced a decrease of the fibre diameter. On the other hand, the orientation of the fibres was obtained with two different collector linear velocities; however, the visual analysis of the SEM images didn't show much fibre alignment.

The thrombogenicity of the structures was assessed with human blood in a perfusion system that mimicked the small diameter fluid dynamics conditions. The fibre with a supposedly higher alignment resulted in a more thrombogenic behaviour; as a matter of fact, the platelets adhered more homogenously and more deeply in the oriented fibre structures.

Finally, the effect of fibre diameter on the platelet deposition was calculated by radioactive labelling of the platelets. The platelet deposition, so the thrombogenicity, resulted to be linearly related to the diameter of the nanofibers of the electrospun surfaces: to a lower diameter structure corresponded a lower platelet deposition.

The structure that resulted in a less thrombogenic behaviour had fibres with an average diameter of 259 nm and resulted in an average platelet deposition of 976 platelets per mm^2, comparable to the platelet deposition on the intact endothelium on an artery, used as positive control.

FUTURE DEVELOPMENTS

In this dissertation, the thrombogenic potential of various nanofibrous electrospun PET structures was assessed; however in order to even better optimise those structures, many experiments need to be done in order to develop the best structure.

First of all, the thrombogenic tests were carried out with a perfusion system that simulated the small diameter fluid dynamics conditions, but the shear stress values change a lot from one small diameter vessel to another one. For that reason, new tests should be done changing the perfusion system conditions.

Secondly, the thrombogenicity of the structures should be measured not only by the platelet deposition count, but also with platelet activation assay like P-selectin secretion and thromboxane A2 production tests.

Thirdly, considering that the relation between the fibre diameter and the platelet deposition is linear, new electrospinning conditions in order to obtain smaller diameter fibres should be investigated.

Finally, PET can be functionalized with artificial polymers, natural polymers and biological polymers in order to improve the thrombogenic resistance, or the endothelial cells spreading on the surface. Thrombogenic tests should be repeated after PET functionalization for a better understanding of the thrombogenic phenomenon.

BIBLIOGRAPHY

Agarwal, S., Wendorff, J.H., & Greiner, A. (2008). Use of electrospinning technique for biomedical applications. *Polymer, 49*(26), 5603-5621. doi: 10.1016/j.polymer.2008.09.014

Amara, U., Rittirsch, D., Flierl, M., Bruckner, U., Klos, A., Gebhard, F., . . . Huber-Lang, M. (2008). Interaction Between the Coagulation and Complement System. Dans J. D. Lambris (Édit.), *Current Topics in Complement II* (vol. 632, p. 68-76): Springer US.

Andersson, J. (2003). *Complement activation triggered by biomaterial surfaces: Mechanisms and regulation.* (Ph. D., Uppsala University, Uppsala).). Tiré de http://urn.kb.se/resolve?urn=urn:nbn:se:uu:diva-3410

Badimon, L., Turitto, V., Rosemark, J.A., Badimon, J.J., & Fuster, V. (1987). Characterization of a tubular flow chamber for studying platelet interaction with biologic and prosthetic materials: deposition of indium 111-labeled platelets on collagen, subendothelium, and expanded polytetrafluoroethylene. *The Journal of laboratory and clinical medicine, 110*(6), 706-718. Tiré de http://ukpmc.ac.uk/abstract/MED/3681113

Bansal, P., Bubel, K., Agarwal, S., & Greiner, A. (2012). Water-stable all-biodegradable microparticles in nanofibers by electrospinning of aqueous dispersions for biotechnical plant protection. *Biomacromolecules, 13*(2), 439-444. doi: 10.1021/bm2014679

Basmadjian, D., Sefton, M.V., & Baldwin, S.A. (1997). Coagulation on biomaterials in flowing blood: some theoretical considerations. *Biomaterials, 18*(23), 1511-1522. doi: 10.1016/s0142-9612(97)80002-6

Baumgarten, P.K. (1971). Electrostatic spinning of acrylic microfibers. *Journal of Colloid and Interface Science, 36*(1), 71-79. doi: 10.1016/0021-9797(71)90241-4

Bergan, J.J., Veith, F.J., Bernhard, V.M., Yao, J.S., Flinn, W.R., Gupta, S.K., . . . Towne, J.B. (1982). Randomization of autogenous vein and polytetrafluorethylene grafts in femoral-distal reconstruction. *Surgery, 92*(6), 921-930. Tiré de http://ukpmc.ac.uk/abstract/MED/6755789

Blanchemain, N., Haulon, S., Martel, B., Traisnel, M., Morcellet, M., & Hildebrand, H.F. (2005). Vascular PET Prostheses Surface Modification with Cyclodextrin Coating: Development of a New Drug Delivery System. *European Journal of Vascular and Endovascular Surgery, 29*(6), 628-632. doi: 10.1016/j.ejvs.2005.02.020

Bland, M. (1995). *An introduction to medical statistics* (2e éd.): Oxford University Press.

Blockmans, D., Deckmyn, H., & Vermylen, J. (1995). Platelet actuation. *Blood Reviews, 9*(3), 143-156. doi: 10.1016/0268-960x(95)90020-9

Brown, B.N., Ratner, B.D., Goodman, S.B., Amar, S., & Badylak, S.F. (2012). Macrophage polarization: An opportunity for improved outcomes in biomaterials and regenerative medicine. *Biomaterials, 33*(15), 3792-3802. doi: 10.1016/j.biomaterials.2012.02.034

Campbell, J.H., Efendy, J.L., & Campbell, G.R. (1999). Novel vascular graft grown within recipient's own peritoneal cavity. *Circulation Research, 85*(12), 1173-1178. doi: 10.1161/01.res.85.12.1173

Casper, C.L., Stephens, J.S., Tassi, N.G., Chase, D.B., & Rabolt, J.F. (2003). Controlling surface morphology of electrospun polystyrene fibers: Effect of humidity and molecular weight in the electrospinning process. *Macromolecules, 37*(2), 573-578. doi: 10.1021/ma0351975

Colman, R.W. (1984). Surface-mediated defense reactions. The plasma contact activation system. *The Journal of Clinical Investigation, 73*(5), 1249-1253. doi: 10.1172/jci111326

Crapo, P.M., & Wang, Y. (2010). Physiologic compliance in engineered small-diameter arterial constructs based on an elastomeric substrate. *Biomaterials, 31*(7), 1626-1635. doi: 10.1016/j.biomaterials.2009.11.035

De Vrieze, S., Van Camp, T., Nelvig, A., Hagström, B., Westbroek, P., & De Clerck, K. (2009). The effect of temperature and humidity on electrospinning. *Journal of Materials Science, 44*(5), 1357-1362. doi: 10.1007/s10853-008-3010-6

Deitzel, J.M., Kleinmeyer, J., Harris, D., & Beck Tan, N.C. (2001). The effect of processing variables on the morphology of electrospun nanofibers and textiles. *Polymer, 42*(1), 261-272. doi: 10.1016/s0032-3861(00)00250-0

Demir, M.M., Yilgor, I., Yilgor, E., & Erman, B. (2002). Electrospinning of polyurethane fibers. *Polymer, 43*(11), 3303-3309. doi: 10.1016/s0032-3861(02)00136-2

Diener, J.L., Daniel Lagasse, H.A., Duerschmied, D., Merhi, Y., Tanguay, J.F., Hutabarat, R., . . . Schaub, R. (2009). Inhibition of von Willebrand factor-mediated platelet activation and thrombosis by the anti-von Willebrand factor A1-domain aptamer ARC1779. *Journal of thrombosis and haemostasis : JTH, 7*(7), 1155-1162. doi: 10.1111/j.1538-7836.2009.03459.x

Dieval, F., Khoffi, F., Mir, R., Chaouch, W., Le Nouen, D., Chakfe, N., & Durand, B. (2012). Long-term biostability of PET vascular prostheses. *International Journal of Polymer Science, 2012*. doi: 10.1155/2012/646578

Dimitrievska, S., Maire, M., Diaz-Quijada, G.A., Robitaille, L., Ajji, A., Yahia, L.H., . . . Bureau, M.N. (2011). Low thrombogenicity coating of nonwoven PET fiber structures for vascular grafts. *Macromolecular Bioscience, 11*(4), 493-502. doi: 10.1002/mabi.201000390

Eda, G., Liu, J., & Shivkumar, S. (2007). Solvent effects on jet evolution during electrospinning of semi-dilute polystyrene solutions. *European Polymer Journal, 43*(4), 1154-1167. doi: 10.1016/j.eurpolymj.2007.01.003

FitzGerald, G.A. (1991). Mechanisms of platelet activation: Thromboxane A2 as an amplifying signal for other agonists. *The American Journal of Cardiology, 68*(7), B11-B15. doi: 10.1016/0002-9149(91)90379-y

Fong, H., Chun, I., & Reneker, D.H. (1999). Beaded nanofibers formed during electrospinning. *Polymer, 40*(16), 4585-4592. doi: 10.1016/s0032-3861(99)00068-3

Formhals, A. (1934). US Brevet n^{o} 1975504. Washington, DC: U.S. Patent and Trademark Office.

Gawaz, M., Langer, H., & May, A.E. (2005). Platelets in inflammation and atherogenesis. *The Journal of Clinical Investigation, 115*(12), 3378-3384. doi: 10.1172/jci27196

Gorbet, M.B., & Sefton, M.V. (2004). Biomaterial-associated thrombosis: roles of coagulation factors, complement, platelets and leukocytes. *Biomaterials, 25*(26), 5681-5703. doi: 10.1016/j.biomaterials.2004.01.023

Hadač, J., Slobodian, P., & Sáha, P. (2007). Volume relaxation in amorphous and semicrystalline PET. *Journal of Materials Science, 42*(11), 3724-3731. doi: 10.1007/s10853-006-0378-z

Hadjizadeh, A., Ajji, A., & Bureau, M.N. (2011). Nano/micro electro-spun polyethylene terephthalate fibrous mat preparation and characterization. *Journal of the Mechanical Behavior of Biomedical Materials, 4*(3), 340-351. doi: 10.1016/j.jmbbm.2010.10.014

Heidenreich, P.A., Trogdon, J.G., Khavjou, O.A., Butler, J., Dracup, K., Ezekowitz, M.D., . . . Woo, Y.J. (2011). Forecasting the future of cardiovascular disease in the United States. *Circulation, 123*(8), 933-944. doi: 10.1161/CIR.0b013e31820a55f5

Horbett, T.A. (1993). Chapter 13 Principles underlying the role of adsorbed plasma proteins in blood interactions with foreign materials. *Cardiovascular Pathology, 2*(3, Supplement), 137-148. doi: 10.1016/1054-8807(93)90054-6

Italiano, J.E., Jr., Mairuhu, A.T., & Flaumenhaft, R. (2010). Clinical relevance of microparticles from platelets and megakaryocytes. *Current opinion in hematology, 17*(6), 578-584. doi: 10.1097/MOH.0b013e32833e77ee

Kang, Y., Park, C., Kim, J., & Kang, T. (2007). Application of electrospun polyurethane web to breathable water-proof fabrics. *Fibers and Polymers, 8*(5), 564-570. doi: 10.1007/bf02875881

Khorasani, M.T., & Shorgashti, S. (2006). Fabrication of microporous thermoplastic polyurethane for use as small-diameter vascular graft material. I. Phase-inversion method. *Journal of Biomedical Materials Research Part B: Applied Biomaterials, 76B*(1), 41-48. doi: 10.1002/jbm.b.30363

Klinger, M.H.F. (1997). Platelets and inflammation. *Anatomy and Embryology, 196*(1), 1-11. doi: 10.1007/s004290050075

Klinkert, P., Post, P.N., Breslau, P.J., & van Bockel, J.H. (2004). Saphenous vein versus PTFE for above-knee femoropopliteal bypass. A review of the literature. *European Journal of Vascular and Endovascular Surgery, 27*(4), 357-362. doi: 10.1016/j.ejvs.2003.12.027

Lee, J.S., Choi, K.H., Ghim, H.D., Kim, S.S., Chun, D.H., Kim, H.Y., & Lyoo, W.S. (2004). Role of molecular weight of atactic poly(vinyl alcohol) (PVA) in the structure and properties of PVA nanofabric prepared by electrospinning. *Journal of Applied Polymer Science, 93*(4), 1638-1646. doi: 10.1002/app.20602

Liang, D., Hsiao, B.S., & Chu, B. (2007). Functional electrospun nanofibrous scaffolds for biomedical applications. *Advanced Drug Delivery Reviews, 59*(14), 1392-1412. doi: 10.1016/j.addr.2007.04.021

Ma, Z., Kotaki, M., Yong, T., He, W., & Ramakrishna, S. (2005). Surface engineering of electrospun polyethylene terephthalate (PET) nanofibers towards development of a new

material for blood vessel engineering. *Biomaterials, 26*(15), 2527-2536. doi: 10.1016/j.biomaterials.2004.07.026

Ma, Z., Mao, Z., & Gao, C. (2007). Surface modification and property analysis of biomedical polymers used for tissue engineering. *Colloids and Surfaces B: Biointerfaces, 60*(2), 137-157. doi: 10.1016/j.colsurfb.2007.06.019

Megelski, S., Stephens, J.S., Chase, D.B., & Rabolt, J.F. (2002). Micro- and nanostructured surface morphology on electrospun polymer fibers. *Macromolecules, 35*(22), 8456-8466. doi: 10.1021/ma020444a

Merhi, Y., King, M., & Guidoin, R. (1997). Acute thrombogenicity of intact and injured natural blood conduits versus synthetic conduits: neutrophil, platelet, and fibrin(ogen) adsorption under various shear-rate conditions. *Journal of Biomedical Materials Research, 34*(4), 477-485.

Mo, X.M., Xu, C.Y., Kotaki, M., & Ramakrishna, S. (2004). Electrospun P(LLA-CL) nanofiber: a biomimetic extracellular matrix for smooth muscle cell and endothelial cell proliferation. *Biomaterials, 25*(10), 1883-1890. doi: 10.1016/j.biomaterials.2003.08.042

National Institutes of Health. (2012). ImageJ. Tiré de http://rsb.info.nih.gov/ij/

O'Brien, J.R. (1990). Shear-induced platelet aggregation. *The Lancet, 335*(8691), 711-713. doi: 10.1016/0140-6736(90)90815-m

Ondarçuhu, T., & Joachim, C. (1998). Drawing a single nanofibre over hundreds of microns. *EPL (Europhysics Letters), 42*(2), 215. Tiré de http://stacks.iop.org/0295-5075/42/i=2/a=215

Papaioannou, T.G., & Stefanadis, C. (2005). Vascular wall shear stress: basic principles and methods. *Hellenic journal of cardiology : HJC = Hellenike kardiologike epitheorese, 46*(1), 9-15.

Paszkowiak, J.J., & Dardik, A. (2003). Arterial wall shear stress: Observations from the bench to the bedside. *Vascular and Endovascular Surgery, 37*(1), 47-57. doi: 10.1177/153857440303700107

Pevec, W.C., Darling, R.C., L'Italien, G.J., & Abbott, W.M. (1992). Femoropopliteal reconstruction with knitted, nonvelour dacron versus expanded polytetrafluoroethylene. *Journal of Vascular Surgery, 16*(1), 60-65. doi: 10.1016/0741-5214(92)90418-8

Qin, X.-H., & Wang, S.-Y. (2006). Filtration properties of electrospinning nanofibers. *Journal of Applied Polymer Science, 102*(2), 1285-1290. doi: 10.1002/app.24361

Ramakrishna, S. (2005). *An introduction to electrospinning and nanofibers*: World Scientific.

Rand, M., Lock, J., van't Veer, C., Gaffney, D., & Mann, K. (1996). Blood clotting in minimally altered whole blood. *Blood, 88*(9), 3432-3445. Tiré de http://bloodjournal.hematologylibrary.org/content/88/9/3432.abstract

Reneker, D.H., Yarin, A.L., Fong, H., & Koombhongse, S. (2000). Bending instability of electrically charged liquid jets of polymer solutions in electrospinning. *Journal of Applied Physics, 87*(9), 4531-4547. doi: 10.1063/1.373532

Rinder, H., Bonan, J., Rinder, C., Ault, K., & Smith, B. (1991). Dynamics of leukocyte-platelet adhesion in whole blood. *Blood, 78*(7), 1730-1737. Tiré de http://bloodjournal.hematologylibrary.org/content/78/7/1730.abstract

Roger, V.L., Go, A.S., Lloyd-Jones, D.M., Adams, R.J., Berry, J.D., Brown, T.M., . . . Wylie-Rosett, J. (2011). Heart disease and stroke statistics—2011 update: A report from the American Heart Association. *Circulation, 123*(4), e18-e209. doi: 10.1161/CIR.0b013e3182009701

Shenoy, S.L., Bates, W.D., Frisch, H.L., & Wnek, G.E. (2005). Role of chain entanglements on fiber formation during electrospinning of polymer solutions: good solvent, non-specific polymer–polymer interaction limit. *Polymer, 46*(10), 3372-3384. doi: 10.1016/j.polymer.2005.03.011

Son, W.K., Youk, J.H., Lee, T.S., & Park, W.H. (2004). The effects of solution properties and polyelectrolyte on electrospinning of ultrafine poly(ethylene oxide) fibers. *Polymer, 45*(9), 2959-2966. doi: 10.1016/j.polymer.2004.03.006

Song, Y., Feijen, J., Grijpma, D.W., & Poot, A.A. (2011). Tissue engineering of small-diameter vascular grafts: A literature review. *Clinical Hemorheology and Microcirculation, 49*(1), 357-374. doi: 10.3233/ch-2011-1486

Suh, T.S. (2007). *World Congress on Medical Physics and Biomedical Engineering 2006: August 27 - September 1, 2006, COEX Seoul, Korea : "Imaging the Future Medicine"*. Tiré de http://books.google.ca/books?id=YUl9bz-om1kC

Taylor, G. (1969). Electrically driven jets. *Proceedings of the Royal Society of London. A. Mathematical and Physical Sciences, 313*(1515), 453-475. doi: 10.1098/rspa.1969.0205

Translation Bureau. Government of Canada. (2012a). Hemocompatibility. *Termium Plus*. Tiré de http://www.termiumplus.gc.ca/tpv2alpha/alpha-eng.html?lang=eng&i=&index=alt&srchtxt=HEMOCOMPATIBILITY

Translation Bureau. Government of Canada. (2012b). Thrombogenicity. *Termium Plus*. Tiré de http://www.termiumplus.gc.ca/tpv2alpha/alpha-eng.html?lang=eng&i=&index=alt&srchtxt=THROMBOGENICITY

Tripatanasuwan, S., Zhong, Z., & Reneker, D.H. (2007). Effect of evaporation and solidification of the charged jet in electrospinning of poly(ethylene oxide) aqueous solution. *Polymer, 48*(19), 5742-5746. doi: 10.1016/j.polymer.2007.07.045

van der Kamp, K.W.H.J., Hauch, K.D., Feijen, J., & Horbett, T.A. (1995). Contact activation during incubation of five different polyurethanes or glass in plasma. *Journal of Biomedical Materials Research, 29*(10), 1303-1306. doi: 10.1002/jbm.820291018

Vogler, E.A. (1998). Structure and reactivity of water at biomaterial surfaces. *Advances in Colloid and Interface Science, 74*(1–3), 69-117. doi: 10.1016/s0001-8686(97)00040-7

Vroman, L., Adams, A., Fischer, G., & Munoz, P. (1980). Interaction of high molecular weight kininogen, factor XII, and fibrinogen in plasma at interfaces. *Blood, 55*(1), 156-159. Tiré de http://bloodjournal.hematologylibrary.org/content/55/1/156.abstract

Wendorff, J.H., Agarwal, S., & Greiner, A. (2012). *Electrospinning: Materials, processing, and applications*. Hoboken, NJ: Wiley.

World Health Organisation. (2012). Cardiovascular disease. Tiré de http://www.who.int/cardiovascular_diseases/en/

Xie, J., Li, X., & Xia, Y. (2008). Putting Electrospun Nanofibers to Work for Biomedical Research. *Macromolecular Rapid Communications, 29*(22), 1775-1792. doi: 10.1002/marc.200800381

Yuan, X., Zhang, Y., Dong, C., & Sheng, J. (2004). Morphology of ultrafine polysulfone fibers prepared by electrospinning. *Polymer International, 53*(11), 1704-1710. doi: 10.1002/pi.1538

Zhang, M. (2004). Biocompatibility of materials. Dans D. Shi (Édit.), *Biomaterials and Tissue Engineering* (p. 111-117). Berlin: Springer.

Zhao, S., Wu, X., Wang, L., & Huang, Y. (2004). Electrospinning of ethyl–cyanoethyl cellulose/tetrahydrofuran solutions. *Journal of Applied Polymer Science, 91*(1), 242-246. doi: 10.1002/app.13196

Zong, X., Kim, K., Fang, D., Ran, S., Hsiao, B.S., & Chu, B. (2002). Structure and process relationship of electrospun bioabsorbable nanofiber membranes. *Polymer, 43*(16), 4403-4412. doi: 10.1016/s0032-3861(02)00275-6

Zucchelli, A., Focarete, M.L., Gualandi, C., & Ramakrishna, S. (2011). Electrospun nanofibers for enhancing structural performance of composite materials. *Polymers for Advanced Technologies, 22*(3), 339-349. doi: 10.1002/pat.1837